J Occup Health 2014; 56: 28–38

Journal of Occupational Health

An Integrative Study of the Genetic, Social and Environmental Determinants of Chronic Kidney Disease Characterized by Tubulointerstitial Damages in the North Central Region of Sri Lanka

Shanika NANAYAKKARA*[1,10], STMLD SENEVIRATHNA*[1,11], Tilak ABEYSEKERA[2], Rohana CHANDRAJITH[3], Neelakanthi RATNATUNGA[4], EDL GUNARATHNE[5], Junxia YAN[1], Toshiaki HITOMI[1], Eri MUSO[6], Toshiyuki KOMIYA[6], Kouji H. HARADA[1], Wanyang LIU[1], Hatasu KOBAYASHI[1], Hiroko OKUDA[1], Hideyuki SAWATARI[7], Fumihiko MATSUDA[8], Ryo YAMADA[8], Takao WATANABE[7], Hideki MIYATAKA[9], Seiichiro HIMENO[9] and Akio KOIZUMI[1]

[1]Department of Health and Environmental Sciences, Graduate School of Medicine, Kyoto University, Japan, [2]Department of Pharmacology, Faculty of Medicine, University of Peradeniya, Sri Lanka, [3]Department of Geology, Faculty of Science, University of Peradeniya, Sri Lanka, [4]Department of Pathology, Faculty of Medicine, University of Peradeniya, Sri Lanka, [5]Girandurukotte Base Hospital, Sri Lanka, [6]Department of Nephrology and Dialysis, Tazuke Kofukai Medical Research Institute, Kitano Hospital, Japan, [7]Miyagi University of Education, Japan, [8]Center for Genomic Medicine, Graduate School of Medicine, Kyoto University, Japan, [9]Laboratory of Molecular Nutrition and Toxicology, Faculty of Pharmaceutical Sciences, Tokushima Bunri University, Japan, [10]Institute of Dental Research, Westmead Centre for Oral Health, Faculty of Dentistry, The University of Sydney, Australia and [11]School of Computing, Engineering and Mathematics, University of Western Sydney, Australia

Abstract: An Integrative Study of the Genetic, Social and Environmental Determinants of Chronic Kidney Disease Characterized by Tubulointerstitial Damages in the North Central Region of Sri Lanka: Shanika NANAYAKKARA, *et al.* Department of Health and Environmental Sciences, Graduate School of Medicine, Kyoto University—Objectives: Previous investigations on chronic kidney disease of unknown etiology characterized by tubulointerstitial damages (CKDu) in the North Central Region (NCR) of Sri Lanka have supported the involvement of social, environmental and genetic factors in its pathogenesis. **Methods:** We conducted a social-environmental-and-genetic epidemiology study on a male population in NCR to investigate the genetic and environmental contributors. We recruited 311 case-series patients and 504 control candidates. Of the 504 control candidates, 218 (43%) were eliminated because of the presence of hypertension, proteinuria, high HbA1c, high serum creatinine or high alpha-1 microglobulin in urine. **Results and Discussion:** None of 18 metals measured (μg/l) in urine, including Cd, As and Pb, showed significantly higher concentrations in cases compared with controls. As speciation results showed that 75–80% of total urinary As was in the form of arsenobetaine, which is non-toxic to humans. None of the metal concentrations in drinking water samples exceeded guideline values. A genome-wide association study (GWAS) was conducted to determine the genetic contributors. The GWAS yielded a genome-wide significant association with CKDu for a single nucleotide polymorphism (SNP; rs6066043; $p=5.23 \times 10^{-9}$ in quantitative trait locus analysis; $p=3.73 \times 10^{-8}$ in dichotomous analysis) in *SLC13A3* (sodium-dependent dicarboxylate transporter member 3). The population attributable fraction and odds ratio for this SNP were 50% and 2.13. Genetic susceptibility was identified as the major risk factor for CKDu. However, 43% of the apparently healthy male

Received Aug 2, 2013; Accepted Oct 4, 2013
Published online in J-STAGE Dec 18, 2013
Correspondence to: A. Koizumi, Department of Health and Environmental Sciences, Graduate School of Medicine, Kyoto University, Konoe-cho, Yoshida, Sakyo-ku, Kyoto 606-8501, Japan (e-mail: koizumi.akio.5v@kyoto-u.ac.jp)
**These two authors contributed equally to this work.*
Supplementary data can be viewed in the online version of this paper in the J-STAGE website.

population suffers from non-communicable diseases, suggesting their possible influence on CKDu progression.
(J Occup Health 2014; 56: 28–38)

Key words: Arsenic, Chronic kidney disease, Farming, Fluoride, High blood pressure, *SLC13A3*

Based on data from renal clinics at tertiary care hospitals, the prevalence of chronic kidney disease (CKD) in areas in and around the North Central Province of Sri Lanka (hereafter referred as the North Central Region, NCR) has been speculated to be relatively high[1]. Local health professionals claim that diabetes mellitus, hypertension and other identifiable causes of CKD are not responsible for CKD in this region. Since its pathogenesis is entirely unknown, it is designated as CKD of unknown etiology (CKDu).

In the previous study in NCR, we found that tubulointerstitial fibrosis was identified as the dominant histopathological lesion in CKDu[2], which supports opinions of local pathologists. In accordance with the pathological characteristics, we found that a tubular marker, alpha-1-microglobulin (A1M), was elevated in CKDu cases and was a sensitive marker for screening the population and diagnosing early-stage CKDu patients[3]. In addition to these findings, we found that family history was a risk factor and observed familial clustering in some families, suggesting the involvement of genetic factors[3]. Over the last few years, research to explain tubulointerstitial damages focusing on the involvement of environmental factors, such as Cd, As, and fluoride, has been reported, but not confirmed[4–6]. An epidemiological study revealed male paddy farmer preponderance and association with various life styles[7]. The aim of this study was to comprehensively evaluate the possible involvement of environmental, social, and genetic factors in the pathogenesis of CKDu with tubulointerstitial damages.

Materials and Methods

Ethics statement

This study was approved by the ethics committees of Kyoto University, Japan, and the Faculty of Medicine, University of Peradeniya, Sri Lanka. All human samples, clinical reports, and questionnaire data were obtained after receiving written informed consent, and the study was performed in accordance with the guidelines of the Declaration of Helsinki.

Study populations for environmental and genetic studies

CKDu cases were defined as cases who developed CKDu in the clinical course of tubulointerstitial damages. Thus, we eliminated CKD that can be a secondary complication of diabetes (history of diabetes mellitus and HbA1c >6.5% at the time of diagnosis of CKD) or hypertension (history of chronic and/or severe hypertension at the time of diagnosis of CKD), or other known renal diseases such as autoimmune diseases, glomerular nephritis, Fanconi syndrome or IgA nephropathy (presence of histopathological and immunoflurocence evidence). Previous studies suggested that areas of residence and male sex are strong risk factors for CKDu[2, 3, 5]. Therefore, we selected two areas, Medawachchiya and Girandurukotte, where CKDu has been postulated to be more prevalent, and male sex for this study (Fig. 1A).

Figure 1B shows a schematic representation of the selection methodology for the cases and controls recruited for this study. We invited male CKDu case-series patients (age range, 16–70 years) from a single ethnic group (Sinhalese), who were registered in Medawachchiya and Girandurukotte renal clinics from January 2005 to December 2010. The response rate was about 90%, and these patients were recruited as cases for this study (n=311). Cases were confirmed to have tubulointerstitial damage by either renal biopsy or clinical data; 93% (n=288) were biopsy-proven (interstitial fibrosis with or without interstitial inflammation and negative immunofluorescence for IgG, IgM, IgA, and C3) and 7% (n=23) had serum creatinine >1.2 mg/d*l* and/or A1M >15.5 mg/*l*. In parallel, we used the clinical records to confirm that these patients developed CKDu in the course of tubulointerstitial damage and the cases did not have uncontrolled hypertension or diabetes at the time of initial diagnosis.

With assistance from community administrative leaders, randomly selected apparently healthy Sinhalese males (age range, 16–70 years), who had no past history of hypertension, diabetes mellitus, or renal diseases, were not on treatment for any other disease condition, and had resided in the region for at least 10 years, were invited to participate. The response rate was about 60%. As illustrated in Figure 1B, blood pressure measurement, dipstick test for proteinuria and glycosuria in spot urine samples, HbA1c, serum creatinine, and A1M were used to recruit subjects without undiagnosed hypertension, diabetes, or renal function impairment.

All the selected cases and controls were interviewed using a structured questionnaire to collect personal, occupational, lifestyle-related, food habit-related, and clinical information. Blood samples (10 m*l*) were collected from peripheral veins into K-EDTA tubes. Serum was separated immediately by centrifugation at 3,000 rpm for 10 minutes. Spot urine samples were also collected from all the recruited cases and controls into empty polypropylene tubes.

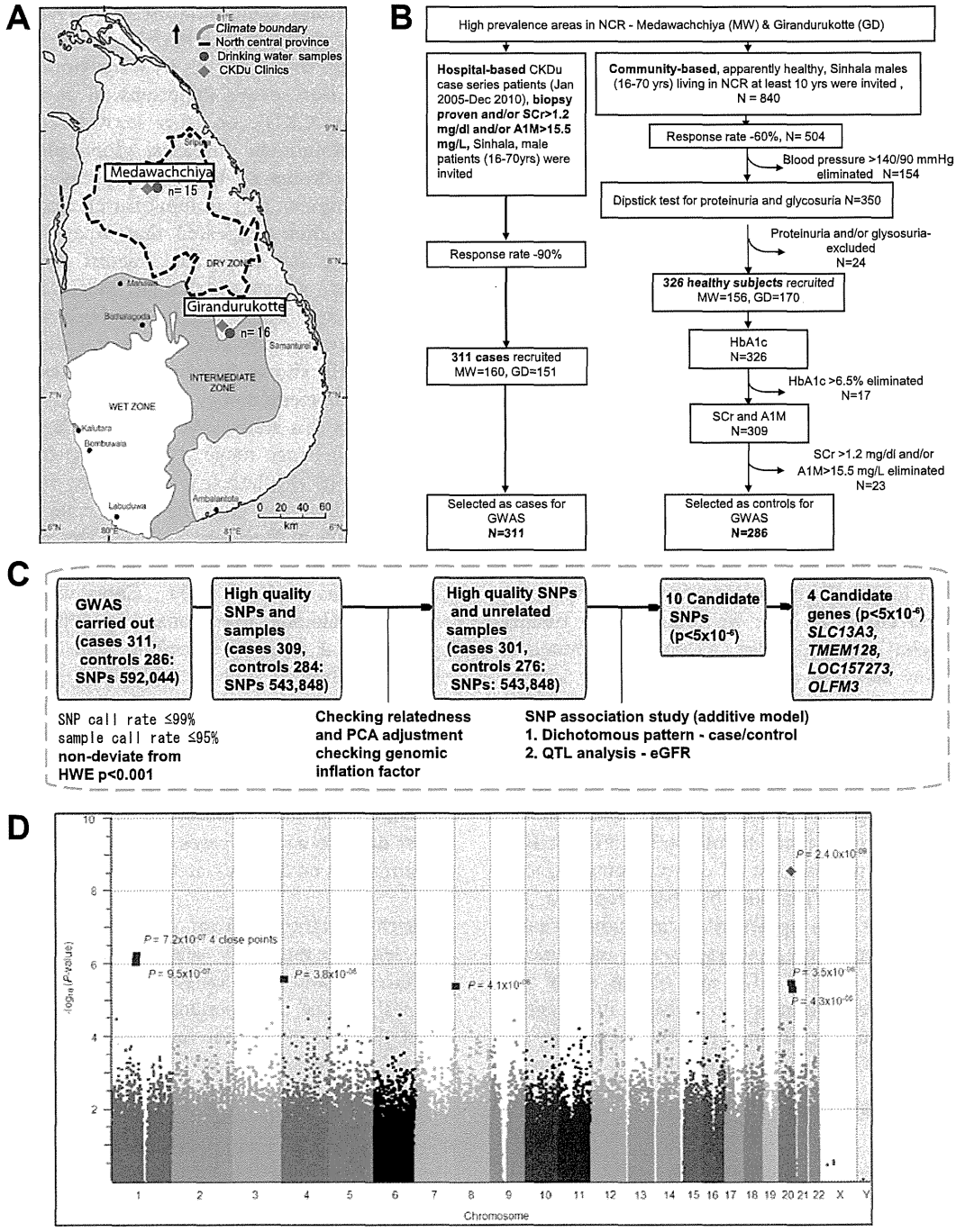

Fig. 1. Study area and design. (A) North Central Province in Sri Lanka and sampling locations. The map shows the locations of the CKDu clinics (Medawachchiya and Girandurukotte) from where the human samples were collected. Water samples were collected from two areas in NCR (Medawachchiya and Girandurukotte).
(B) Flow chart summarizing the selection process for the cases and controls. MW, Medawachchiya; GD, Girandurukotte; SCr, serum creatinine; A1M, alpha-1-microglobulin; GWAS, genome-wide association study.
(C) Study design for the genetic analysis. GWAS, genome-wide association study; HWE, Hardy-Weinberg equation; QTL, quantitative trait locus; eGFR, estimated glomerular filtration rate, PCA, principal component analysis.
(D) Manhattan plot. The Manhattan plot shows the significance of associations for all SNPs. The SNPs are plotted on the X-axis according to their position on each chromosome against the association with the estimated glomerular filtration rate on the Y-axis, shown as the $-\log_{10}(p\text{-value})$. One SNP showing a genome-wide significant association and all SNPs achieving $p<5 \times 10^{-6}$ are shown with their p-values.

Water samples (1 *l* each) were collected into empty polypropylene bottles from drinking water sources in two areas of NCR (Medawachchiya, n=15; Girandurukotte, n=16) (Fig. 1A). The water samples were randomly selected from common drinking water sources in villages with a high incidence of CKDu.

All the drinking water, urine, serum, and whole-blood samples were immediately stored at 4°C and then transferred to −30°C within 6 hours of collection. The samples were shipped to Japan at −20°C and stored at −30°C until analysis.

The estimated glomerular filtration rate (eGFR) was obtained using the modified diet in renal disease (MDRD) formula, i.e. GFR (ml/min/1.73 m^2)=186 × serum creatinine$^{-1.154}$ × (age)$^{-0.203}$ × (0.742 if female), based on the serum creatinine levels[8]. In addition, we conducted a field survey to investigate food habits of the local residents.

Drinking water, serum and urine analyses

Drinking water and urine samples were analyzed for heavy metals using inductively coupled plasma mass spectrometry (ICP-MS). Urinary heavy metals were checked in all subjects recruited for the genome-wide association study (GWAS) (n=597). From the 286 controls, 154 subjects (54%; 77 per area) and from the 311 cases, 176 subjects (57%; 88 per area) were randomly selected for As speciation. Urinary As speciation was carried out using Agilent 1260 HPLC BIO inert, Agilent ICP-MS 7700x (HPLC-ICP-MS). Serum fluoride was analyzed using flow injection analysis with a fluoride ion-selective electrode. Urinary creatinine concentrations, urinary A1M and HbA1c were measured at Special Reference Laboratory (Tokyo, Japan). The detection limits for As species are 0.02 $\mu g/l$ and standard reference materials (Seronorm Trace Elements Urine L-1 and L-2, SERO AS, Billingstad, Norway) were analyzed in every analytical batch. Coefficients of variance (n=26) ranged from 4.2% (Cs) to 42.3% (Ni) in the Urine L-1 analysis and from 3.8% (Tl) to 22.6% (Fe) in the Urine L-2 analysis.

Genome-wide association study and direct sequencing

DNA was extracted from the whole-blood samples using a QIAamp DNA Blood Mini Kit (Qiagen, Chatsworth, CA) for the GWAS. The GWAS was performed on 597 subjects (n=311 for cases; n=286 for controls) using Illumina 500 K Chips (Human 610-Quad-Custom v1.0 DNA Analysis Bead Chip; Illumina, San Diego, CA) according to standard protocols. Prior to the analysis, the data sets were filtered on the basis of the single nucleotide polymorphism (SNP) genotyping call rates (≥99% completeness), sample call rates (≥95%), non-deviation from the Hardy-Weinberg equilibrium (p<0.001), and evidence of cryptic family relationships (Fig. 1C).

Principal component analysis showed no outliers and all subjects were confirmed to be of a single ethnicity (Fig. S1). A quantile-quantile plot revealed that the distribution of observed p values followed the expected distribution (Fig. S2). The inflation factor was calculated to be 1.0. The analyses were based on an additive genetic model. Analyses were performed using SVS version 7.6.10, GoldenHelix software (Golden Helix, Inc., Bozeman, MT, USA). Values of $p<5.0 \times 10^{-8}$ were considered to show genome-wide significance and values of $5 \times 10^{-8}<p<5 \times 10^{-6}$ were considered to show suggestive evidence of an association.

Direct sequencing of the *SLC13A3* gene and *TP53RK* gene including the 5'-UTR, 3'-UTR, exons and 100-bp covering splicing donor and acceptor sites was performed using the Sanger method in eight randomly selected cases and eight randomly selected controls. Information on the primer sequences and PCR conditions will be provided upon request to the corresponding author.

Determination of the numbers of CAA repeats

We determined the numbers of CAA repeats in the 5' promoter region of *SLC13A3* in all cases and controls. The regions around the CAA repeats were amplified by PCR using fluorescently tagged primers (forward, 5'-FAM-AGC CTG GGT AAC AGA GTG AGA-3'; reverse, 5'-TCC CTT TAA GAC CTC ATC ACC-3'). The expected size of PCR products was 215 + 3 n (where n=CAA repeat number). The sizes of amplification products were analyzed by DNA sequencer.

Statistics

Univariate and multiple logistic analyses for demographic factors, past events and life-style related factors were conducted to identify the risk factors. To show the distribution of urinary creatinine levels and each metal parameter, we presented means with standard deviations, medians, minimums, maximums and percentiles (25%, 75%). Some urinary parameters were not normally distributed and we computed the statistical significance of differences between cases and controls using both parametric (Student's t-test) and non-parametric (Kolmogorov-Smirnov) methods. A comparison of serum fluoride levels among different CKD stages (stages 1–5) was made using the Student-Newman-Keuls (SNK) multiple range test. A p value of <0.05 following adjustment by Bonferroni correction, using the number of urinary metal parameters in multiple comparisons, was considered significant. All statistical procedures were performed using STATISTICA 64 (supplied by StatSoft, OK, USA).

Results

Population characteristics and characterization of risk factors

As shown in Figure 1B, we recruited 504 candidate control subjects. Blood pressure measurements eliminated 154 subjects owing to hypertension. A further 24 subjects were eliminated because of proteinuria and/or glycosuria. Seventeen subjects were eliminated owing to high HbA1c levels and 23 subjects were eliminated because of elevated serum creatinine or urinary A1M levels. In total, 43% of the 504 participants were eliminated.

The demographic and clinical characteristics of the selected cases and controls are summarized in Table 1. The CKDu cases were older and had stayed longer in the region than the controls. On average, the subjects in both groups were neither overweight nor underweight. We identified several risk factors (Table S1). The percentage of farmers was significantly higher in the cases (97.1%) than in the controls (69.9%). Some lifestyle-related factors that are commonly associated with farming occupation, such as smoking, betel chewing, tobacco chewing, and history of snake bites were also significantly more common in the cases than in the controls. The presence of CKDu family history was significantly higher in the cases than in the controls. The significant factors ($p<0.05$) identified in univariate analyses were further analyzed using multiple logistic analysis. This analysis revealed that farming, family history of CKDu, tobacco chewing and history of snake bites were independent risk factors (Table 2).

Metal concentrations in drinking water

Metal concentrations in drinking water samples collected from Medawachchiya and Girandurukotte are summarized in Table S2 together with the maximum allowable limits in drinking water recommended by the WHO (http://www.who.int/water_sanitation_health/publications/2011/dwq_guidelines/en/index.html) and/or United States Environmental Protection Agency (http://water.epa.gov/drink/contaminants/index.cfm). We further compared the metal concentrations with the Japanese water quality standards (Ministry of Environment, Japan, 2004; http://www.env.go.jp/en/water/wq/wp.pdf). According to the available recommendations, none of the metals, which have guideline values including nephrotoxic metals such as Cd, As, and Pb, were present at toxic concentrations in the drinking water consumed daily by the CKDu cases in Medawachchiya and Girandurukotte.

Metal concentrations in urine

In Table 3, we presented metal concentrations ($\mu g/l$) in urine in cases and controls. We could not conduct urine analyses for 10 cases and 10 controls due to inadequate sample volume. To decrease false positive rates, a significant level ($p=0.003=0.05/18$) was adjusted by numbers of metals examined (n=18). None of the 18 metal concentrations was higher in urines in cases than in controls, including nephrotoxic metals such as Pb, Cd, As, Ni, V, and Al. Reversely, several metals were higher in controls than in cases ($p<0.001$); Pb, Tl, Cs, Cd, Mo, Sr, Rb, Se, As, Ni, Co, V, and Al. Cases had significantly lower creatinine concentrations in urine (n=301: 0.72 ± 0.53 g/l) than controls (n=276: 1.18 ± 0.70 g/l) ($p<0.0001$), suggesting impaired urine concentration ability due to

Table 1. Demographic and clinical characteristics of the study subjects

Parameter	Cases		Controls		p
	Mean (SD)	Min-Max	Mean (SD)	Min-Max	
n	311	—	286	—	–
Age (yr)	46.6 (9.0)	16–68	41.1 (8.1)	20–59	<0.0001
Duration of stay in NCR (yr)	39.0 (12.3)	7–68	33.1 (12.1)	10–59	<0.0001
Body mass index (kg/m^2)	21.1 (3.4)	13.6–35.7	23.0 (4.3)	15.6–43.7	<0.0001
Blood pressure (systolic) (mmHg)	124.0 (18.9)	65–220	128.0 (10.6)	90–139	0.0013
Blood pressure (diastolic) (mmHg)	71.0 (12.6)	35–125	74.6 (9.0)	47–89	<0.0001
Serum creatinine (mg/dl)	2.12 (1.10)	0.46–11.1	0.88 (0.11)	0.56–1.18	<0.0001
eGFR (ml/min/1.73 m^2)	45.7 (23.1)	5.3–204.3	104.0 (17.0)	67.4–180.9	<0.0001
Urinary alpha-1-microglobulin (mg/l)	65.9 (52.3)	0.1–410.7	1.6 (2.4)	0.1–13.8	<0.0001
Glycated hemoglobin (HbA1c %)	5.5 (0.6)	3.7–9.8*	5.4 (0.5)	2.9–6.5	0.0052
Serum fluoride ($\mu g/l$)	86.4 (51.6)	12.7–367	35.5 (16.2)	9.5–99.0	<0.0001

eGFR, estimated glomerular filtration rate; HbA1c, glycated hemoglobin. *Six cases were diagnosed with diabetes after the diagnosis of CKDu.

Table 2. Multiple logistic analysis for selected demographic factors, life-style related factors and past events

Parameter	Odds ratio (95% CI)	*p*
Farming vs. other occupations	9.17 (20.00–4.18)	<0.0001
Family history of CKDu	2.66 (4.15–1.70)	<0.0001
Tobacco chewing	2.59 (4.02–1.68)	<0.0001
History of snake bites	1.93 (3.16–1.18)	0.0093
History of malaria	1.31 (1.96–0.87)	0.1925
Smoking	1.25 (1.89–0.83)	0.2782
Betel chewing	1.38 (2.38–0.80)	0.2520

CI, confidence interval; CKDu, chronic kidney disease of unknown etiology.

Table 3. Metal concentrations in urine

Meta	Cases ($\mu g/l$) n=301				Controls ($\mu g/l$) n=276				p^a value	p^b value
	Mean (SD)	Geometric Mean	Min–Max	25% / 50% / 75%	Mean (SD)	Geometric Mean	Min–Max	25% / 50% / 75%		
Pb	0.94 (0.89)	0.69	0.05–8.42	0.39 / 0.68 / 1.16	1.88 (2.55)	1.45	0.21–31.8	0.96 / 1.43 / 2.23	<0.001*	<0.001*
Tl	0.18 (0.19)	0.12	0–1.10	0.06 / 0.11 / 0.22	0.38 (0.26)	0.30	0.01–1.73	0.2 / 0.32 / 0.49	<0.001*	<0.001*
Cs	3.09 (2.77)	2.18	0.25–20.3	1.13 / 2.16 / 4.23	5.81 (4.08)	4.57	0.14–23.6	2.92 / 4.87 / 6.99	<0.001*	<0.001*
Cd	0.47 (0.78)	0.25	0.02–7.17	0.11 / 0.25 / 0.52	1.76 (1.89)	0.78	0.03–8.24	0.23 / 0.78 / 3.1	<0.001*	<0.001*
Mo	55.6 (48.9)	38.4	2.36–314	19.4 / 42.6 / 75.9	105 (97.5)	73.7	4.62–972	39.3 / 80.8 / 141	<0.001*	<0.001*
Sr	132 (115)	94.4	8.74–650	55.4 / 97.3 / 172	247 (163)	191	16.1–829	119 / 226 / 332	<0.001*	<0.001*
Rb	1,380 (1,250)	1,020	185–9,860	575 / 1,030 / 1,780	2,360 (1620)	1,900	130–9,900	1,270 / 1,980 / 2,810	<0.001*	<0.001*
Se	16.8 (15.0)	11.5	0.37–101	6.11 / 12.8 / 22.5	29.8 (20.0)	23.6	2.00–124	15.9 / 25.4 / 38.2	<0.001*	<0.001*
As	33.2 (37.5)	20.3	1.49–259	10.2 / 21.8 / 40.6	44.4 (43.5)	29.6	1.22–277	18.1 / 30.2 / 55.4	<0.001*	<0.001*
Zn	374 (322)	279	36.2–2,130	163 / 276 / 476	428 (453)	304	24.6–4,210	180 / 315 / 522	0.1	>0.10
Cu	16.2 (15.5)	12.0	0.99–153	7.70 / 11.9 / 19.3	15.7 (11.6)	12.7	1.41–116	8.39 / 13.1 / 19.9	0.628	>0.10
Ni	4.04 (3.06)	3.11	0.18–23.2	1.79 / 3.18 / 5.27	5.52 (4.19)	4.51	0.45–37.9	3.07 / 4.54 / 6.92	<0.001*	<0.001*
Co	0.42 (0.41)	0.30	0.04–3.30	0.17 / 0.32 / 0.48	0.55 (0.48)	0.42	0.03–3.28	0.26 / 0.42 / 0.65	<0.001*	<0.001*
Fe	10.8 (24.4)	5.83	0.04–280	3.37 / 5.89 / 10.4	11.5 (46.9)	6.82	1.36–773.18	4.3 / 6.59 / 9.86	0.817	<0.025
Mn	0.68 (1.14)	0.51	0.07–19.0	0.34 / 0.53 / 0.75	0.84 (1.97)	0.59	0.08–31.9	0.38 / 0.60 / 0.90	0.213	<0.05
Cr	0.19 (0.30)	0.12	0–3.62	0.08 / 0.13 / 0.19	0.24 (0.78)	0.15	0.01–12.63	0.10 / 0.15 / 0.23	0.291	<0.005
V	0.46 (0.31)	0.36	0.02–1.66	0.24 / 0.41 / 0.61	0.67 (0.31)	0.58	0.01–2.67	0.46 / 0.68 / 0.86	<0.001*	<0.001*
Al	4.60 (3.61)	3.70	0.31–30.0	2.54 / 3.67 / 5.52	6.60 (8.51)	4.95	0.03–114.98	3.37 / 4.78 / 7.39	<0.001*	<0.001*

p^a, *p* value calculated by *t*-test; p^b, *p* value calculated by Kolmogorov-Smirnov (non-parametric) test; *Significant by Bonferroni correction (p=0.05/18=0.003).

CKDu. Thus, we also investigated the metal concentrations in urine adjusted by urinary creatinine levels (Table S3). Creatinine-adjusted As, Zn, Cu, Co, Mn, and Al concentrations in urine were significantly higher in cases than in controls (p<0.05/18=0.003) in both parametric and non-parametric analyses (Table S3). However, it should be addressed that irrespective of the adjustment for creatinine level, urinary Cd concentration was significantly higher in controls than in cases (Table 3 and S3), indicating that Cd is not a causative factor for CKDu.

In terms of As, our results were much lower than the reported concentrations in As-contaminated areas in countries such as Bangladesh and Taiwan[10, 11]. However, the total As concentrations were relatively higher than the concentrations observed in some uncontaminated areas in Europe, the United States, and Canada (http://www.hc-sc.gc.ca/ewh-semt/alt_formats/hecs-sesc/pdf/pubs/contaminants/chms-ecms/report-rapport-eng.pdf)[12, 13]. Therefore, we conducted speciation to investigate a possibility that modest contamination with As may be associated with CKDu. A total of 330 urine samples were duplicated and analyzed at two independent laboratories for total As and As speciation. The sum of arsenic speciation components (As-III, As-V, MMA, DMA, AB, Table 4) measured by HPLC ICP-MS nicely matched the total As levels measured by ICP-MS (Table 3 and

Table 4. As speciation results unadjusted and adjusted by urinary creatinine levels

Component	Controls (n=154)			Cases (n=176)			p^a value	p^b value
	mean (SD)	Min–Max	25% / 50% / 75%	mean (SD)	Min–Max	25% / 50% / 75%		
Unadjusted for creatinine								
As (III) ($\mu g/l$)	0.71 (0.94)	<0.02–9.71	0.14 / 0.59 / 1.05	0.39 (2.16)	<0.02–28.0	<0.02 / 0.10 / 0.27	0.095	<0.05
As (V) ($\mu g/l$)	0.22 (0.36)	<0.02–3.42	0 / 0.14 / 0.27	0.14 (0.24)	<0.02–2.42	<0.02 / 0.10 / 0.18	<0.05	>0.1
MMA ($\mu g/l$)	0.57 (0.57)	<0.02–5.09	0.23 / 0.46 / 0.73	0.56 (0.58)	<0.02–4.49	0.21 / 0.37 / 0.62	0.859	>0.1
DMA ($\mu g/l$)	7.83 (7.75)	0.49–65.9	3.63 / 5.94 / 9.21	6.39 (7.40)	0.41–46.4	2.16 / 4.60 / 7.19	0.087	<0.05
AB ($\mu g/l$)	33.0 (35.7)	<0.02–215	10.0 / 20.5 / 41.0	25.5 (33.4)	0.17–227	6.96 / 15.2 / 28.8	<0.05	<0.05
Total As ($\mu g/l$)	42.4 (38.6)	1.62–237	16.5 / 29.4 / 52.5	33.0 (37.8)	1.77–234	9.78 / 22.2 / 40.8	<0.05	<0.05
UCr ($\mu g/l$)	1.19 (0.7)	0.06–3.87	0.68 / 1.08 / 1.50	0.72 (0.53)	0.06–4.11	0.34 / 0.59 / 0.97	<0.05	<0.05
Adjusted for creatinine								
As (III) (μg/g-Cr)	0.82 (1.36)	ND–14.5	0.18 / 0.45 / 1.23	0.77 (5.25)	ND–69.4	ND / 0.18 / 0.42	0.404	<0.05
As (V) (μg/g-Cr)	0.28 (0.52)	ND–5.12	ND / 0.12 / 0.33	0.35 (0.88)	ND–9.08	ND / 0.14 / 0.34	<0.05	<0.1
MMA (μg/g-Cr)	0.54 (0.40)	ND–2.60	0.3 / 0.48 / 0.68	0.92 (0.67)	ND–3.91	0.47 / 0.72 / 1.19	<0.05	<0.05
DMA (μg/g-Cr)	7.05 (6.02)	1.14–58.7	3.98 / 5.42 / 8.41	9.43 (6.06)	1.52–35.5	5.44 / 7.97 / 11.8	<0.05	<0.05
AB (μg/g-Cr)	29.0 (31.5)	ND–258	11.1 / 21.6 / 33.7	40.2 (44.9)	1.08–275	13.4 / 24.5 / 45.9	<0.05	<0.10
Total As (μg/g-Cr)	37.7 (32.7)	4.1–270	18.8 / 30.9 / 43.4	51.7 (47.6)	6.04–303	21.1 / 36.2 / 59.2	0.095	<0.05

*Significant by Bonferroni correction. p^a, p value calculated by t-test; p^b, p value calculated by Kolmogorov-Smirnov (non-parametric) test. MMA, Monomethylarsonic acid; DMA, Dimethylarsinic acid; AB, Arsenobetaine; UCr, urinary creatinine; ND, not detected.

Table 4, and Fig. S3: R^2=0.97, p<0.0001). As speciation results revealed that 75–80% of total urinary As in both cases and controls was in the form of arsenobetaine (Table 4), which is non-toxic. Adjustment with creatinine showed that total arsenic concentration (μg/g-Cr) in urine was greater in cases than in controls. However, the difference of the total arsenic concentration was mostly attributable to the difference in arsenobetaine fraction (Table 4). Hata *et al* (2007) reported that the median total urinary arsenic level of a Japanese healthy male adult is 141.3 $\mu g/l$ and the arsenobetaine level is 61.3 $\mu g/l$; these levels are about three times higher than those of CKDu cases[9]. The modestly elevated levels of arsenobetaine in urine are in accord with the common habit of eating dry fish in these areas, as confirmed by the field study. Typical signs of chronic As exposure, such as skin keratosis and pigmentation, were observed in neither the cases nor the controls.

Fluoride concentration in serum

An inverse relationship was observed between the eGFR and the serum fluoride concentration (Fig. S4). However, the eGFR stratified analysis demonstrated that serum fluoride levels were not different between cases and controls (Table S4) with eGFR >60 ml/min/1.73 m^2. Moreover, the serum fluoride concentrations in the majority of the unaffected and early-stage CKDu patients were below the reported upper normal concentration of 50 $\mu g/l$[14]. Thus, we concluded that higher serum fluoride is a result of lowered eGFR (impaired renal function) and not the primary cause of CKDu.

GWAS

A total of 543,848 GWAS SNPs in 577 samples were left after the quality control process for the associations test with the eGFR (quantitative trait locus (QTL) analysis) or the affected status (dichotomous analysis) (Fig. 1C). A genome-wide view of the single point association data is shown in Fig. 1D.

A summary of the association results (QTL analysis and dichotomous analysis, with and without age adjustment) for 10 candidate SNPs located in four genes is shown in Table 5 (see also Fig. 1D). The top hit that reached the genome-wide significance level ($p<5 \times 10^{-8}$) in both the QTL analysis and dichotomous analysis was rs6066043 (G>A), which is localized on the *SLC13A3* gene encoding sodium-dependent dicarboxylate transporter 3 ($p=5.23 \times 10^{-9}$ for age-adjusted QTL analysis; $p=3.73 \times 10^{-8}$ for age-adjusted dichotomous analysis). The population attributable fraction and odds ratio for this SNP were 50% and 2.13. The allele frequencies for this SNP vary among populations. The G allele is more common among European populations (88% G allele frequency), while it is found in less than 50% of individuals in Asian populations (HapMap data). In the present study, the G allele frequencies in the cases and controls were 77% and 62%, respectively.

Table 5. Ten SNPs with significant and suggestive evidence of associations identified in the genome-wide association study

	SNP	Chr:position	Alleles	Gene	Distance	MAF (number)	MAF (number)	Slope (OR)	*p* value for QTL analysis (dichotomous analysis)	
						Cases	Controls		Without age adjustment	With age adjustment
1	rs17126268	1:102498987	T>C	*OLFM3*	264	0.03 (Wild=281, HT=19, Homo=1)	0.10 (Wild=225, HT=48, Homo=3)	17.42 (2.78)	7.19×10^{-7} (1.58×10^{-5})	5.29×10^{-6} (9.64×10^{-5})
2	rs7539242	1:102499390	G>A	*OLFM3*	264	0.03 (Wild=281, HT=19, Homo=1)	0.10 (Wild=225, HT=48, Homo=3)	17.42 (2.78)	7.19×10^{-7} (1.58×10^{-5})	5.29×10^{-6} (9.64×10^{-5})
3	rs12135261	1:102501863	C>T	*OLFM3*	266	0.03 (Wild=281, HT=19, Homo=1)	0.10 (Wild=225, HT=48, Homo=3)	17.42 (2.78)	7.19×10^{-7} (1.58×10^{-5})	5.29×10^{-6} (9.64×10^{-5})
4	rs12120258	1:102507539	G>T	*OLFM3*	272	0.03 (Wild=281, HT=19, Homo=1)	0.10 (Wild=225, HT=48, Homo=3)	17.42 (2.78)	7.19×10^{-7} (1.58×10^{-5})	5.29×10^{-6} (9.64×10^{-5})
5	rs12140211	1:102512105	C>T	*OLFM3*	276	0.07 (Wild=259, HT=41, Homo=1)	0.14 (Wild=203, HT=68, Homo=5)	13.71 (2.00)	9.54×10^{-7} (9.21×10^{-5})	1.48×10^{-5} (7.59×10^{-4})
6	rs2980098	4:4303857	A>G	*TMEM128*	13	0.37 (Wild=120, HT=138, Homo=43)	0.49 (Wild=73, HT=138, Homo=65)	9.11 (1.61)	3.80×10^{-6} (1.00×10^{-4})	2.16×10^{-6} (1.22×10^{-4})
7	rs10099338	8:9295149	A>G	*LOC157273*	65	0.05 (Wild=273, HT=28, Homo=0)	0.10 (Wild=221, HT=53, Homo=2)	13.28 (2.04)	4.05×10^{-6} (1.00×10^{-4})	4.50×10^{-4} (4.33×10^{-3})
8	rs1004571	20:44711576	A>G	*SLC13A3*	Intragenic	0.32 (Wild=32, HT=129, Homo=140)	0.44 (Wild=51, HT=142, Homo=83)	7.98 (1.63)	4.33×10^{-6} (2.78×10^{-5})	6.23×10^{-5} (1.73×10^{-4})
9	rs6066043	20:44721860	G>A	*SLC13A3*	Intragenic	0.23 (Wild=175, HT=113, Homo=13)	0.38 (Wild=104, HT=132, Homo=40)	12.17 (2.13)	2.40×10^{-9} (1.13×10^{-8})	5.23×10^{-9} (3.73×10^{-8})
10	rs4810537	20:44740335	A>G	*SLC13A3*	Intragenic	0.33 (Wild=32, HT=137, Homo=132)	0.45 (Wild=54, HT=142, Homo=80)	8.02 (1.60)	3.47×10^{-6} (2.78×10^{-5})	6.08×10^{-5} (2.67×10^{-4})

Chr, chromosome; MAF, minor allele frequency; OR, odds ratio; HT, heterozygous; SNP, single nucleotide polymorphism; QTL, quantitative trait locus. *p* values for both the QTL analysis and dichotomous analysis are shown. Reference sequence: GRCh36 (2006).

Since the SNP rs6066043 is located in the intergene region of *SLC13A3* and *TP53RK* (Fig. S5), it is hard to explain the functional impairment by this SNP. We thus screened for variants in these two genes. Direct sequencing was conducted for all coding exons and the 5'UTR and 3'UTR for these two genes. The results of direct sequencing are shown in Table S5. We identified variations in the CAA repeat number in the 5' promoter region, 14.6 Kb upstream of exon 1 of *SLC13A3* ($p<0.01$). Minor allele frequencies of other variants did not seem to differ in cases and controls. Thus, the sizes of the CAA repeat expansion were determined using fluorescently tagged primers in all cases and controls and this revealed variation in the CAA repeat expansion from $(CAA)_{10}$ to $(CAA)_{18}$. We investigated the association between repeat numbers and CKDu. Considering $(CAA)_{15}$ as the wild-type, an odds ratio was calculated for the repeat polymorphism (Table S6) to be 1.6, being smaller than odds ratio of rs6066043 (2.13) (Table 5). No significant difference in mean eGFR was observed among various CAA repeat combinations (Table S6). Thus, we considered that (CAA) repeats were not a causative variant for CKDu.

The GWAS study revealed three other genes with suggestive evidence ($5 \times 10^{-8}<p<5 \times 10^{-6}$) of an association: *OLFM3*, *TMEM128* and *LOC157273* (Table 5). However, *OLFM3* can be discarded because it is an olfactory gene.

Discussion

This is the first comprehensive study addressing both the genetic, social, and environmental contributors of CKDu with tubulointerstitial damages in NCR of Sri Lanka. Ecological investigations in the present study confirmed the absence of nephrotoxic heavy metal contamination in drinking water. We found that the SNP rs6066043 of *SLC13A3* loads discernible risk of CKDu in the local population as indicated by a large population attributable risk of 50%. It should also be addressed that occupation, family history of CKD, tobacco chewing, and history of snakebites were also identified as independent risk factors.

None of 18 metals had urinary concentrations ($\mu g/l$) greater in cases than in controls. Only when adjusted to the urinary creatinine levels (μg/g-cre), it was found that the Zn, Cu, Co, Mn, and Al levels in urine were higher in cases than in controls. However, comparison of these levels with those in other populations is difficult due to the limited availability of published data. We considered that due to the impaired urine concentration ability in cases, those apparent elevations of urine concentrations for some metals might emerge by adjustment with creatinine levels. Further studies are needed to verify the individual and combined effects of these metal parameters on CKDu.

It is worthwhile mentioning that urinary concentrations of total As levels in cases and controls were suggestive of modest exposure to As. Thus, we conducted speciation of As compounds in urine. Speciation revealed that arsenobetaine is the major As compound, suggesting that seafood is the major sources of As[13]. The high urinary As concentrations in countries like Japan and Korea were found to result from the high amounts of seafood intake, and As speciation studies showed high proportions of arsenobetaine in urine, which is non toxic[9, 15]. A field survey on the food habits of the population in NCR also supports regular intake of dried sea fish which is likely to be the source of high urinary arsenobetaine levels.

It is worth highlighting the fact that some studies have reported a possible relationship between As exposure and CKD[16, 17]. Hsueh *et al.* (2009) reported a positive association between urinary total As concentration and CKD for the first time in Taiwan, and the total As concentrations in their study population closely resemble the observations in the present study (total mean urinary As in the CKD group and healthy controls: 31.95 and 20.71 versus 50.3 and 39.4 μg/gCr, respectively)[17]. However, the dominant component of total As was arsenobetaine in this study, but dimethylarsinic acid in the Taiwan study. Urinary Cd levels in controls were higher than those in cases, suggesting a minimal involvement of Cd in CKDu. The Cd levels reported in this study are comparable to other published data[18, 19].

The present study revealed that a common genetic variant close to *SLC13A3* is associated with CKDu. *SLC13A3* encodes the high-affinity sodium dicarboxylate transporter 3 located in the basolateral membranes of human renal proximal tubules, liver, brain, and placenta[20]. On the other hand, *TP53RK*, encodes a protein, TP53-regulated kinase, which is a serine/threonine protein kinase[21] and functions in a *P53* signal pathway. *SLC13A3* has been identified as one of the most sensitive marker genes for predicting the clinical course to end-stage renal disease in type 2 diabetes mellitus and has an association with blood pressure[22, 23]. Recently, *SLC13A3* was identified as one of the 43 genes that can be used in protein expression signatures to predict progressive renal fibrosis in mice, and was suggested to be a potentially useful molecular predictor for CKD progression in humans[24]. *SLC13A3* has also been shown to play a role in the accumulation of Hg-thiol conjugates in the basolateral membrane vesicles in proximal tubular cells in the rat[25]. Those pieces of evidence strongly support that *SLC13A3* is more likely mechanistically associated

with CKD rather than *TP53RK*. However, further studies are needed to explain a mechanism by which CKDu is associated with rs6066043.

It was interesting to note that 43% of the apparently healthy male population, most of whom were farmers, had, at least, one undiagnosed non communicable disease, mainly high blood pressure. Mendis *et al.* (1988) reported that the prevalence of high blood pressure among Sri Lankans is one of the highest reported in the world, and Wijewardene *et al* (2005) reported that the area in Sri Lanka with the highest prevalence of high blood pressure is the Uva province[26, 27]. One of our study areas (Girandurukotte) is located in this province. Therefore, it is likely that undiagnosed hypertension may accelerate CKDu progression. Even in one of our previous studies, we found hypertension as a risk factor for CKDu progression[26].

Some limitations of this study warrant mention. We used the eGFR based on the MDRD formula rather than using the direct glomerular filtration rate, since it was not feasible to measure the direct glomerular filtration rate in this setting. However, the MDRD formula is not validated for the Sri Lankan population. Owing to the discrepancies present in the validated MDRD formulas for other Asian populations, we could not use these coefficients for this population[29–32]. A smaller sample size without replication evidence may decrease the robustness of the results, and we have planned to incorporate it in the next stage of this study. Although we confirm the farmer preponderance among CKDu patients, this finding needs cautious interpretation. Given that we selected patients by a case-series method to eliminate possible biases, there may be selection bias in selecting controls. We eliminated 43% of controls due to undiagnosed non-communicable diseases, most of them were farmers. Such an elimination of a large portion of the population from the control candidates suggests that local farmers have less chance to access medical care or preventive care than controls with other occupations. Thus, our conclusion on being a farmer as a risk of CKDu is very likely confounded by the accessibility to medical care or public health services. On the other hand, the elimination of such subjects from control candidates strengthened our genetic analysis. Because we primarily aimed to determine genetic factors for tubulointerstitial damages, we selected cases who developed CKDu in the course of primary tubulointerstitial damages without hypertension or diabetes mellitus or other comorbidities. To unify the selection criteria, controls should be selected with the same backgrounds. Applying the same backgrounds made our genetic analysis for tubulointerstitial damages scientifically sound. If we included controls with hypertension or other morbidities, phenotypic heterogeneity between cases and controls may contaminate our study.

In conclusion, our results do not support the involvement of a founder mutation or single heavy metal in the pathogenesis of CKDu. However, the present study found a significant SNP in *SLC13A3* with an odds ratio of 2.13 and a 50% population attributable fraction, indicating major genetic susceptibility to CKDu. Thus, further study is warranted to elucidate causal link of the SNP rs6066043 with CKDu.

Acknowledgments: We thank Dr Meiko Takahashi (Kyoto University) for support in performing the GWAS, and the staff of the Medawachchiya and Girandurukotte renal clinics for their assistance with the sampling program. The authors would like to acknowledge the Special Coordination Funds for Promoting Science and Technology from the Ministry of Education, Culture, Sports, Science and Technology in Japan. The funding agency had no role in the study design, data collection and analysis, decision to publish, or preparation of the manuscript.

References

1) Athuraliya TN, Abeysekera DT, Amerasinghe PH, Kumarasiri PV, Dissanayake V. Prevalence of chronic kidney disease in two tertiary care hospitals: high proportion of cases with uncertain etiology. Ceylon Med J 2009; 54: 23–5.
2) Nanayakkara S, Komiya T, Ratnatunga N, et al. Tubulointerstitial damage as the major pathological lesion in endemic chronic kidney disease among farmers in North Central Province of Sri Lanka. Environ Health Prev Med 2012; 17: 213–21.
3) Nanayakkara S, Senevirathna ST, Karunaratne U, et al. Evidence of tubular damage in the very early stage of chronic kidney disease of uncertain etiology in the North Central Province of Sri Lanka: a cross-sectional study. Environ Health Prev Med 2012; 17: 109–17.
4) Bandara JM, Senevirathna DM, Dasanayake DM, Herath V, Abeysekara T, Rajapaksha KH. Chronic renal failure among farm families in cascade irrigation systems in Sri Lanka associated with elevated dietary cadmium levels in rice and freshwater fish (Tilapia). Environ Geochem Health 2008; 30: 465–78.
5) Chandrajith R, Nanayakkara S, Itai K, et al. Chronic kidney diseases of uncertain etiology (CKDue) in Sri Lanka: geographic distribution and environmental implications. Environ Geochem Health 2011; 33: 267–78.
6) Jayasumana MACS, Paranagama PA, Amarasinghe MD, et al. Possible link of Chronic arsenic toxicity with chronic kidney disease of unknown etiology. J

Nat Sci Res 2011; 13: 64–73.
7) Athuraliya NTC, Abeysekera TDJ, Amerasinghe PH, et al. Uncertain etiologies of proteinuric-chronic kidney disease in rural Sri Lanka. Kidney Int 2011; 80: 1212–21.
8) Kooman JP. Estimation of renal function in patients with chronic kidney disease. J Magn Reson Imaging 2009; 30: 1341–6.
9) Hata A, Endo Y, Nakajima Y, et al. HPLC-ICP-MS speciation analysis of arsenic in urine of Japanese subjects without occupational exposure. J Occup Health 2007; 49: 217–23.
10) Chen Y, van Geen A, Graziano JH, et al. Reduction in urinary arsenic levels in response to arsenic mitigation efforts in Araihazar, Bangladesh. Environ Health Perspect 2007; 115: 917–23.
11) Chen JW, Chen HY, Li WF, et al. The association between total urinary arsenic concentration and renal dysfunction in a community-based population from central Taiwan. Chemosphere 2011; 84: 17–24.
12) Caldwell KL, Jones RL, Verdon CP, Jarrett JM, Caudill SP, Osterloh JD. Levels of urinary total and speciated arsenic in the US population: National Health and Nutrition Examination Survey 2003-2004. J Expo Sci Environ Epidemiol 2009; 19: 59–68.
13) Saoudi A, Zeghnoun A, Bidondo ML, et al. Urinary arsenic levels in the French adult population: the French National Nutrition and Health Study, 2006-2007. Sci Total Environ 2012; 433: 206–15.
14) Joshi S, Hlaing T, Whitford GM, Compston JE. Skeletal fluorosis due to excessive tea and toothpaste consumption. Osteoporos Int 2011; 22: 2557–60.
15) Lee JW, Lee CK, Moon CS, et al. Korea National Survey for Environmental Pollutants in the Human Body 2008: heavy metals in the blood or urine of the Korean population. Int J Hyg Environ Health 2012; 215: 449–57.
16) Zheng LY, Umans JG, Tellez-Plaza M, et al. Urine arsenic and prevalent albuminuria: evidence from a population-based study. Am J Kidney Dis 2013; 61: 385–94.
17) Hsueh YM, Chung CJ, Shiue HS, et al. Urinary arsenic species and CKD in a Taiwanese population: a case-control study. Am J Kidney Dis 2009; 54: 859–70.
18) Huang M, Choi SJ, Kim DW, et al. Evaluation of factors associated with cadmium exposure and kidney function in the general population. Environ Toxicol 2013; 28: 563–70.
19) Batariova A, Spevackova V, Benes B, Cejchanova M, Smid J, Cerna M. Blood and urine levels of Pb, Cd and Hg in the general population of the Czech Republic and proposed reference values. Int J Hyg Environ Health 2006; 209: 359–66.
20) Pajor AM. Molecular properties of the SLC13 family of dicarboxylate and sulfate transporters. Pflugers Arch 2006; 451: 597–605.
21) Miyoshi A, Kito K, Aramoto T, Abe Y, Kobayashi N, Ueda N. Identification of CGI-121, a novel PRPK (p53-related protein kinase)-binding protein. Biochem Biophys Res Commun 2003; 303: 399–405.
22) Bento JL, Palmer ND, Zhong M, et al. Heterogeneity in gene loci associated with type 2 diabetes on human chromosome 20q13.1. Genomics 2008; 92: 226–34.
23) Simino J, Shi G, Arnett D, Broeckel U, Hunt SC, Rao DC. Variants on chromosome 6p22.3 associated with blood pressure in the HyperGEN study: follow-up of FBPP quantitative trait loci. Am J Hypertens 2011; 24: 1227–33.
24) Ju W, Eichinger F, Bitzer M, et al. Renal gene and protein expression signatures for prediction of kidney disease progression. Am J Pathol 2009; 174: 2073–85.
25) Lash LH, Hueni SE, Putt DA, Zalups RK. Role of organic anion and amino acid carriers in transport of inorganic mercury in rat renal basolateral membrane vesicles: influence of compensatory renal growth. Toxicol Sci 2005; 88: 630–44.
26) Mendis S, Ranasinghe P, Dharmasena BD. Prevalence of hypertension in Sri Lanka. A large population study in the central province. Public Health 1988; 102: 455–62.
27) Wijewardene K, Mohideen MR, Mendis S, et al. Prevalence of hypertension, diabetes and obesity: baseline findings of a population based survey in four provinces in Sri Lanka. Ceylon Med J 2005; 50: 62–70.
28) Senevirathna L, Abeysekera T, Nanayakkara S, et al. Risk factors associated with disease progression and mortality in chronic kidney disease of uncertain etiology: a cohort study in Medawachchiya, Sri Lanka. Environ Health Prev Med 2012; 17: 191–8.
29) Praditpornsilpa K, Townamchai N, Chaiwatanarat T, et al. The need for robust validation for MDRD-based glomerular filtration rate estimation in various CKD populations. Nephrol Dial Transplant 2011; 26: 2780–5.
30) Imai E, Horio M, Nitta K, et al. Estimation of glomerular filtration rate by the MDRD study equation modified for Japanese patients with chronic kidney disease. Clin Exp Nephrol 2007; 11: 41–50.
31) Ma YC, Zuo L, Chen JH, et al. Modified glomerular filtration rate estimating equation for Chinese patients with chronic kidney disease. J Am Soc Nephrol 2006; 17: 2937–44.
32) Matsuo S, Imai E, Horio M, et al. Revised equations for estimated GFR from serum creatinine in Japan. Am J Kidney Dis 2009; 53: 982–92.

Environmental Science & Technology

Article

pubs.acs.org/est

^{137}Cs Trapped by Biomass within 20 km of the Fukushima Daiichi Nuclear Power Plant

Akio Koizumi,*[,†] Tamon Niisoe,[†] Kouji H. Harada,[†] Yukiko Fujii,[†] Ayumu Adachi,[†] Toshiaki Hitomi,[†] and Hirohiko Ishikawa*[,‡]

[†]Department of Health and Environmental Sciences, Graduate School of Medicine, Kyoto University, Kyoto 606-8501, Japan

[‡]Research Division of Atmospheric and Hydrospheric Disasters, Disaster Prevention Research Institute, Kyoto University, Uji 611-0011, Japan

Supporting Information

ABSTRACT: Analysis of ^{137}Cs trapped in biomass in highly contaminated zones is crucial in predicting the long-term fate of ^{137}Cs following the explosion at the Fukushima Daiichi Nuclear Power Plant. We surveyed forest 20−50 km from the plant in July and September 2011 to evaluate ^{137}Cs trapped in biomass within 20 km of the plant. We determined the ambient dose rate and collected forest soils and twigs at 150 sampling points. Removability from the canopy was evaluated by washing leaves and branches with water and organic solvents. The biomass of the forest canopy was then calculated. ^{137}Cs fallout was simulated with an atmospheric transport model. The modeled dose rate agreed with observations (n = 24) (r = 0.62; p < 0.01). Washing experiments demonstrated that unremovable portions accounted for 53.9 ± 6.4% of ^{137}Cs trapped by deciduous canopy (n = 4) and 59.3 ± 13.8% of ^{137}Cs trapped by evergreen canopy (n = 10). In total, it was estimated that 74.5 × 10^{12} Bq was trapped by canopy in the forest within the no-go zone, with 44.2 × 10^{12} Bq allocated to unremovable portions, and that 0.86% of the total release was trapped in biomass as of September 2011.

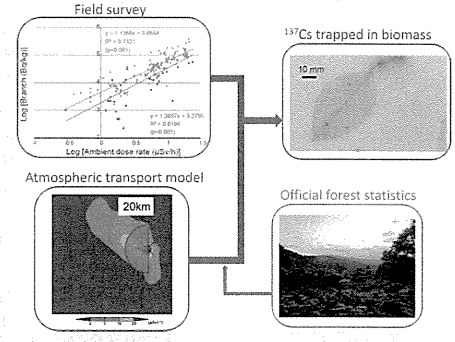

INTRODUCTION

Following the Tohoku earthquake and tsunami of March 11, 2011, there were explosions at the Fukushima Daiichi Nuclear Power Plant (DNPP) on March 15, which released massive quantities of radionuclides into the atmosphere. The total amount of ^{137}Cs released into the atmosphere has been estimated to be approximately 8.6 × 10^{15} Bq.[1] More than 70% of Fukushima Prefecture (Figure 1) in northern Japan is covered by forest, and the majority of radioactivity fell on this forest.

The fates of radionuclides in forest are complicated and not well-understood. Dynamics of ^{137}Cs in forest can be divided into two phases: acute (0−3 years) and late (3+ years) phases.[2] In the acute phase, radionuclides are captured by the forest canopy. In the late phase, radionuclides enter the recycling process through absorption from soil, redistribution in the forest ecosystem, and immobilization in tree biomass. Once ^{137}Cs has entered the recycling process of the forest ecosystem, ^{137}Cs disappears only at the rate of its radioactive decay with a half-life of 30 years, despite radionuclides in the soil slowly departing the ecological system through heavy precipitation and runoff.[2]

After the explosions at the DNPP, the Japanese government set up a no-go zone; i.e., an area within a 20 km radius of the DNPP. It has been speculated that massive amounts of radionuclides have fallen in this area and the land will be

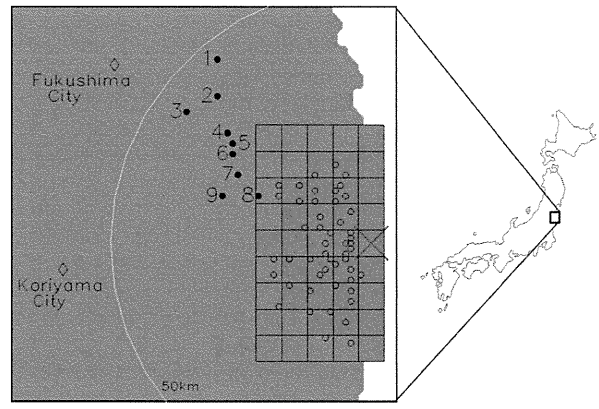

Figure 1. Locations of nine sampling sites. The red "×" indicates the Fukushima DNPP. A total of 29 blue boxes and 50 open circles represent model grid cells and monitoring sites by the Japanese government[15] inside the 20 km zone. Details of the 9 sampling sites and 50 monitoring sites are listed in Tables S1 and S2 of the Supporting Information.

Received: August 2, 2012
Revised: July 18, 2013
Accepted: July 26, 2013
Published: July 26, 2013

contaminated heavily with radionuclides. Because the area is a no-go zone, few data are available for the acute phase following the Fukushima DNPP explosions, although such data are essential to the prediction of the long-term fate of ^{137}Cs.[2] In the current work, we estimated the fall of radiocesium over the forest in the no-go zone from data obtained in a field survey of the 20−50 km zone of the DNPP. We here report the radiocesium distribution in forest biomass following the Fukushima DNPP explosions as of September 2011.

MATERIALS AND METHODS

Sampling and Determination of Radioactivity. A field survey was conducted in July and September 2011 in forest within the zone 20−50 km from the DNPP, a zone which is referred to as the "emergency evacuation preparation zone" by the Japanese government (Figure 1). We visited nine sampling sites, where we determined the ambient dose rate and collected soil and twigs of deciduous and evergreen trees in the forest (see Table S1 of the Supporting Information). The ambient dose rate was determined about 1 m above the ground at each sampling point using an ionization survey meter (ICS-331, Hitachi Aloka Medical, Ltd., Tokyo, Japan). A soil core (5 cm in diameter and 5 cm deep) was taken from the ground surface at each site by embedding a steel cylinder vertically into the ground. In total, 150 samples were collected, and they are listed in Table S1 of the Supporting Information.

Removability was evaluated by washing each sample portion of trees with water and then with a mixture of organic solvents.[3] We selected trees with contamination greater than 5.0×10^4 Bq/kg to eliminate the effects of the background level of ^{137}Cs. Each 1 g portion cut out from the point was washed in 10 mL of ultrapure water ($\geq$18 MΩ cm) for 10 min with sonication (40 kHz) in an ultrasonic washing bath (ASU-3 M ASONE, Tokyo, Japan). To remove radionuclides adsorbed by resin, the portion was then washed in 10 mL of a mixture of tetrahydrofuran and toluene (1:1) for 1 min with sonication in the ultrasonic washing bath. Removability was determined as the removed radioactivity divided by the total activity before washing with ultrapure water and the mixture of tetrahydrofuran and toluene. Radiometric analysis of the washing solution was carried out to evaluate the recovery of washing experiments. The time course of removed radioactivity at 1, 3, and 10 min was assessed for three deciduous trees and six evergreen trees. A washing experiment with organic solvent followed by water was also conducted to validate the quantitative removal of radiocesium. Three independent washing experiments were conducted for each sample, and the mean values of the removability were taken for each sample.

Autoradiography images of leaves and needles were taken to visualize the radioactivity. An imaging plate (BAS-IP MS 2040, Fuji Film) was exposed for 16 h to leaves and needles at 25 °C. Autoradiography was carried out with a fluorescent image analyzer (FLA2000, Fuji Film, Tokyo, Japan). Images of samples before and after washing were compared, employing the method described below. However, the imaging scanner system automatically adjusted the contrast of images, and the images are therefore only qualitative. Thus, densities of images are not proportional to the radioactivities.

Radiometric determinations were performed using a low-background high-purity germanium detector with high resolution at the Radioisotope Research Center of Kyoto University and a multichannel analyzer (4096 channels, range of 0−3000 keV, MCA8000, Princeton Gamma Technologies, Princeton, NJ). Aliquots from each sample were weighed and sealed in cylindrical plastic containers (outer diameter of 55 mm and height of 55 mm). Branchwood samples were vertically aligned at the center of a container using filling spacers. Leave samples were folded and placed at the center of a container. To confirm homogeneity of samples, samples were analyzed twice at different positions. Characteristic γ-ray energies were monitored to identify and quantify the radiocesium (^{134}Cs, 604.7 keV; ^{137}Cs, 661.7 keV). The detector was calibrated using a γ-ray reference source from the Japan Radioisotope Association (Tokyo, Japan). Cellulose powder fortified with radiocesium was analyzed in the same manner as branchwood and leave samples to match sample geometry. All radioactivity values were corrected to March 15, 2011, using physical half-lives (^{134}Cs, 2.06 years; ^{137}Cs, 30.1 years).

Estimation of Biomass and Simulation. The total biomass of the canopy within the 20 km radius was calculated using biomass equations[4] and forest statistics officially reported mainly by the Fukushima prefectural authorities.[5] To estimate total biomass, we classified the trees into two groups: deciduous and evergreen. The detail is described in section S1 of the Supporting Information.

The fallout of ^{137}Cs was calculated for each 5 km area using a widely established atmospheric transport model, the Models-3 Community Multiscale Air Quality (CMAQ) modeling system.[6] The computational domain was 440 km wide from west to east and 540 km wide from south to north and included the Fukushima DNPP. The vertical structure had 40 layers constructed with a pressure-based terrain-following coordinate system (i.e., sigma coordinates). The typical depth of the lowest layer was about 40 m. The meteorological fields were computed using version 3.2 of the Weather Research Forecasting (WRF) model,[7] including 3-hly analysis with the mesoscale model of the Japan Meteorological Agency.

We employed an emission scenario taken from Terada et al.[1] that assumed that there was an explosive daytime release on March 15, 2011, when extremely high dose rates up to 11.9 mSv/h were observed at the main gate of the plant after a large explosive sound and vibration in the morning.[8,9] ^{137}Cs was emitted exclusively in the lowest layer at the point corresponding to the Fukushima DNPP. The simulation period was March 11 to April 1, 2011. The removal of ^{137}Cs was mediated by dry and wet deposition.[6] We observed the size distribution of atmospheric ^{134}Cs and ^{137}Cs in Fukushima city in July 2011 and found that the radionuclides mainly belonged to size bins less than 1 μm.[10] The dry deposition velocity depends upon the particle size in general, but size dependency is almost negligible for particles with diameters ranging between 0.05 and 2.0 μm.[11] The mass concentration and radioactivity of airborne particles less than 0.05 μm in diameter are typically negligible because of the extremely small size of the particles.[12] Wet deposition depends upon the precipitation rate rather than the particle size. Therefore, we can discard the effects of the size distribution of particles in both dry and wet deposition. In this work, the particle size was fixed at 1 μm.

The accumulated deposition of ^{137}Cs calculated by the CMAQ modeling system was converted to the air dose rate. We assumed that the radioactivity of ^{134}Cs was equal to that of ^{137}Cs on March 15, 2011[13] and used conversion factors of 5.4×10^{-6} (mSv/h)/(kBq/m^2) for ^{134}Cs and 2.1×10^{-6} (mSv/h)/(kBq/m^2) for ^{137}Cs.[14] Amounts of ^{137}Cs trapped by forest canopy were estimated using the relationships between ambient dose rates and levels in branches or leaves/needles (panels A

dx.doi.org/10.1021/es401422g | Environ. Sci. Technol. 2013, 47, 9612−9618

and B of Figure 2), which were determined from our field survey and sampling measurements. Calculation of total

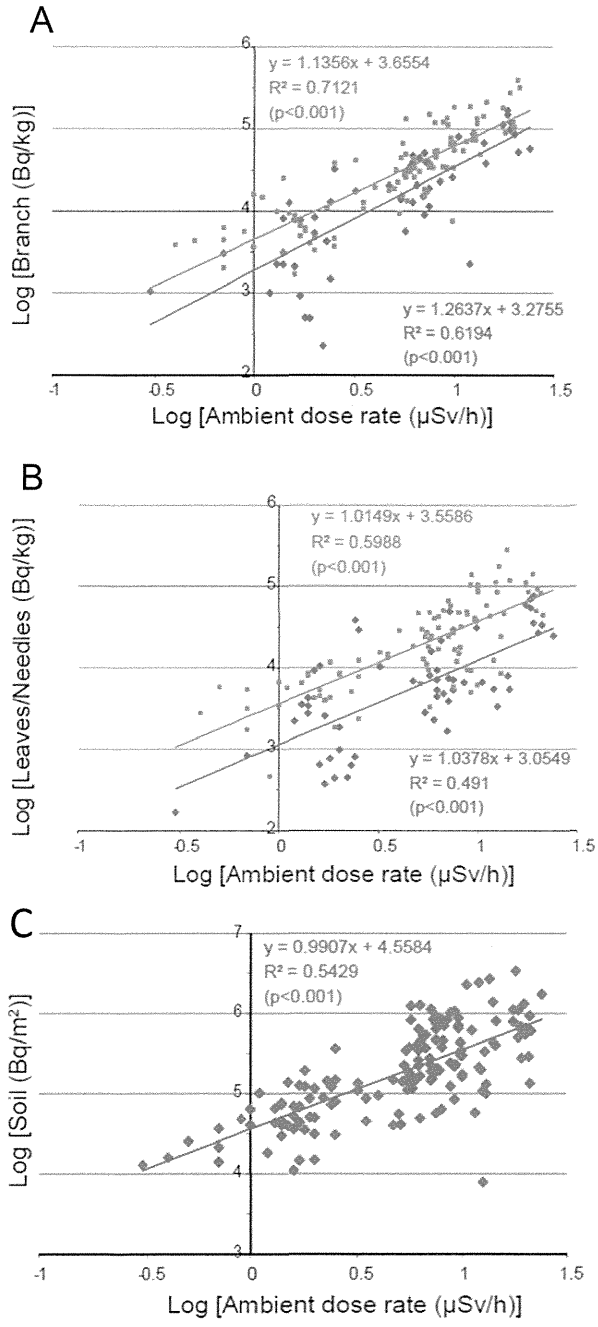

Figure 2. Relationships between ambient dose rates (μSv/h) and radioactivities of biomass/soil: (A) branchwood (Bq/kg), (B) leaves/needles (Bq/kg) and (C) soil (Bq/m^2). Red and blue dots in panels A and B represent evergreen and deciduous trees, respectively.

radioactivity of ^{137}Cs trapped by forest canopy is described further in section S2 of the Supporting Information.

Validation of the Simulation Method. The air dose rate at 50 points within 20 km of the plant was monitored once a week by the Japanese government[15] (Figure 1). The monitoring sites are listed in Table S2 of the Supporting Information. We compared the calculated air dose rates to dose rates observed from May to September 2011, assuming radioactivity of the emitted ^{131}I to be extinct. All data for the monitoring points were binned according to the model resolution into 24 horizontal cells. The fit of the simulated and observed values was evaluated by the fractional difference[16] f averaged for all compared grid points

$$f = \frac{V_{mdl} - V_{obs}}{V_{mdl} + V_{obs}}$$

where V_{mdl} and V_{obs} are the modeled and observed values, respectively. $|f| < 0.33$ indicates an error factor less than 2, which means $V_{obs}/2 < V_{mdl} < V_{obs} \times 2$.

RESULTS AND DISCUSSION

The ratios of ^{134}Cs/^{137}Cs (mean ± standard deviation) were 0.97 ± 0.06 for soil, 0.97 ± 0.09 for branches, and 1.00 ± 0.11 for leaves/needles (see Table S1 of the Supporting Information). The ambient dose rate was significantly correlated ($p < 0.001$) with the radioactivities of both branches and leaves/needles (panels A and B of Figure 2). The ambient dose rate ranged from 0.3 to 24.0 μSv/h and was highly correlated with soil radioactivity (Bq/m^2) ($R^2 = 0.543$; $p < 0.001$) (Figure 2C). The correlation suggests that the higher contamination levels lead to greater amounts of ^{137}Cs in forest biomass. The linear and statistically significant ($p < 0.05$) regression function enabled us to quantitate ^{137}Cs in biomass quasi-quantitatively from the ambient dose rate.

Washing experiments were conducted for 4 deciduous trees and 20 evergreen trees (Table 1). Recovery of ^{137}Cs (activity of washed sample and washing solution divided by activity of prewashed sample) in a water washing experiment was 107 ± 14.4% for leaf samples and 106 ± 16.2% for branchwood samples. Recovery in an organic solvent washing experiment was 105 ± 9.4% for leaf samples and 101 ± 11.6% for branchwood samples. The removability of ^{137}Cs was

Table 1. Removability of ^{137}Cs Determined in a Washing Experiment for Leaves/Needles and Branchwood Portions

trees	relative weight (%)	fraction	percentage (%)
Deciduous Trees (n = 4)			
leaves[a]	9.1	removable	22.2 ± 9.0
		unremovable	77.8 ± 9.0
branchwood[a]	90.9	removable	40.7 ± 3.6
		unremovable	59.3 ± 3.6
canopy[b]	100.0	removable	39.0 ± 5.7
		defoliation	7.1 ± 1.1
		unremovable	53.9 ± 6.4
Evergreen Trees (n = 20)			
needles[a]	44.5	removable	45.1 ± 18.8
		unremovable	54.9 ± 18.8
branchwood[a]	55.5	removable	37.1 ± 18.1
		unremovable	62.9 ± 18.1
canopy[b]	100.0	removable	40.7 ± 13.8
		unremovable	59.34 ± 13.8

[a]Averages ± standard deviations (SDs) were calculated for means of the samples. The mean for each sample is taken over three independent washing experiments. [b]The value for each sample was obtained by adding values for leaves and branches using relative weights (%).

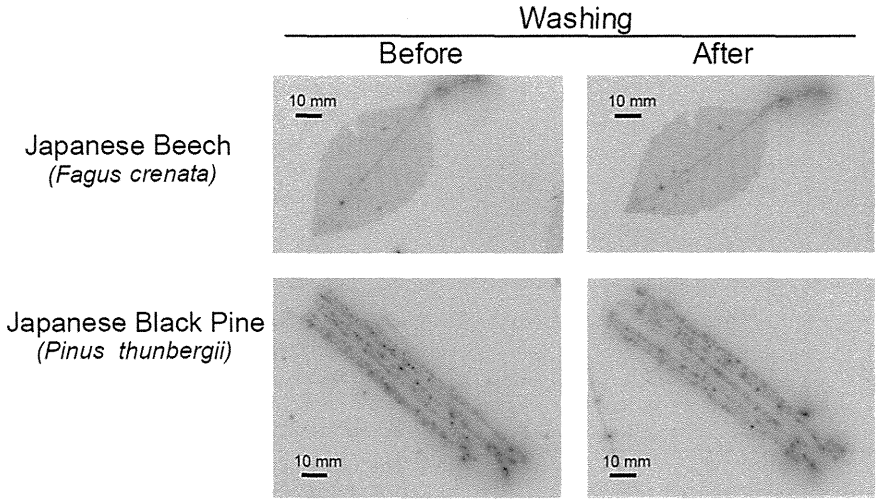

Figure 3. Autoradiographs of leaves/needles. Films were exposed to leaves/needles for 16 h. Samples were randomly selected. Before washing, a small debris of leaves was scattered on an imaging plate, which showed radioactivity outside the leaves. At the left corner of the image of the washed Japanese black pine, there was one needle apart from other needles (see Figure S1 of the Supporting Information). The imaging scanner system automatically adjusted the contrast of the images, and the images are only a qualitative representation. Thus, sensitivities for individual images are different, and thus, densities cannot be compared to each other.

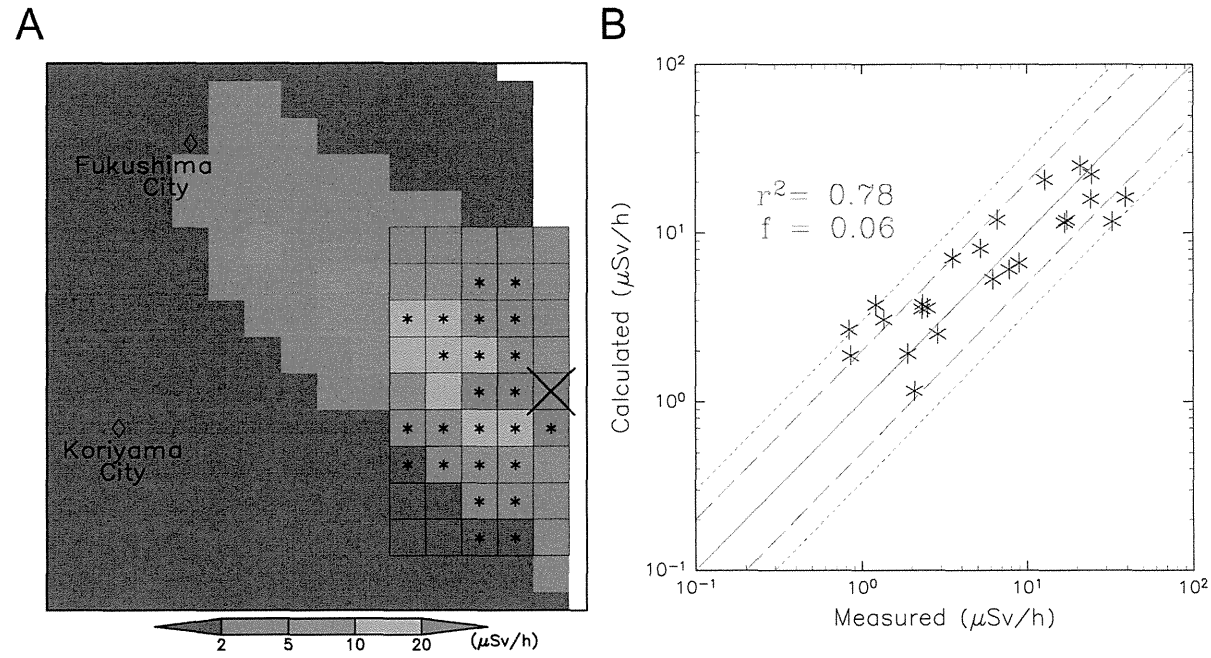

Figure 4. (A) Distribution of the calculated air dose rate (μSv/h). A total of 24 model grid cells used for comparison to observations are indicated by asterisks. (B) Comparison of observations and calculations averaged from May to September 2011 at monitoring points within 20 km of the Fukushima DNPP. The dose rate is corrected to March 15. Agreement is indicated by a correlation coefficient r^2 of 0.78 ($p = 1.4 \times 10^{-8}$) and an averaged fractional difference f of 0.06. The solid line indicates a perfect fit between observations and calculations, and the two dashed lines and two dotted lines indicate error factors of 2 and 3, respectively.

determined in a washing experiment for leaves/needles and branchwood portions (Table 1). More than 60% of the trapped radioactivity was associated with unremovable fractions. These values were comparable to those in a washing experiment with organic solvent followed by water (deciduous trees, 32.1 ± 8.7 and 21.9 ± 8.5% for branchwood and leaf, respectively; evergreen trees, 36.3 ± 15.5 and 33.7 ± 19.0% for branchwood and leaf, respectively). Removal proportions of ^{137}Cs at 1, 3, and 10 min were compatible (deciduous trees, 9.0 ± 5.7, 14.6 ± 8.6, and 16.2 ± 5.2%; evergreen trees, 17.8 ± 10.4, 21.6 ± 12.8, and 22.8 ± 14.5%, respectively). Therefore, easily detachable ^{137}Cs seemed to be removed within 10 min. Unremovable portions of the total canopy were estimated using relative weights. Unremovable portions accounted for 53.9% of all fractions for deciduous trees, assuming all leaves to be

dx.doi.org/10.1021/es401422g | Environ. Sci. Technol. 2013, 47, 9612−9618

Table 2. ^{137}Cs Radioactivity Trapped by Twigs and Estimation of ^{137}Cs Trapped by Biomass within 20 km

				^{137}Cs (Bq)							
biomass	estimated volume (kg)	estimated Bq in the fraction	fraction	estimate	95% PI[a] upper	95% PI[a] lower	upper deposition case	lower deposition case	lower removable case	total upper limit	total lower limit
				Deciduous Trees							
leaves	7.5×10^{7}	9.0×10^{11}	removable	2.0×10^{11}	1.9×10^{12}	2.1×10^{10}	6.0×10^{11}	6.6×10^{10}	1.0×10^{11}	2.9×10^{12}	6.9×10^{9}
			unremovable	7.0×10^{11}	6.7×10^{12}	7.2×10^{10}	2.1×10^{12}	2.3×10^{11}	8.0×10^{11}	2.3×10^{13}	2.4×10^{10}
branch wood	3.3×10^{8}	1.2×10^{13}	removable	4.7×10^{12}	6.3×10^{13}	3.5×10^{11}	1.4×10^{13}	1.6×10^{12}	2.4×10^{12}	9.5×10^{13}	1.2×10^{11}
			unremovable	6.9×10^{12}	9.2×10^{13}	5.2×10^{11}	2.1×10^{13}	2.3×10^{12}	9.3×10^{12}	3.7×10^{14}	1.7×10^{11}
canopy	4.1×10^{8}	1.3×10^{13}	removable + defoliation	5.6×10^{12}	7.2×10^{13}	4.5×10^{11}	1.7×10^{13}	1.9×10^{12}	3.3×10^{12}	1.2×10^{14}	1.5×10^{11}
			unremovable	6.9×10^{12}	9.2×10^{13}	5.2×10^{11}	2.1×10^{13}	2.3×10^{12}	9.3×10^{12}	3.7×10^{14}	1.7×10^{11}
				Evergreen Trees							
needles	5.9×10^{8}	2.0×10^{13}	removable	9.2×10^{12}	4.7×10^{13}	1.8×10^{12}	2.8×10^{13}	3.1×10^{12}	4.6×10^{12}	7.0×10^{13}	6.1×10^{11}
			unremovable	1.1×10^{13}	5.7×10^{13}	2.2×10^{12}	3.4×10^{13}	3.7×10^{12}	1.6×10^{13}	2.4×10^{14}	7.4×10^{11}
branch wood	7.1×10^{8}	4.2×10^{13}	removable	1.5×10^{13}	7.5×10^{13}	3.2×10^{12}	4.6×10^{13}	5.1×10^{12}	7.7×10^{12}	1.1×10^{14}	1.1×10^{12}
			unremovable	2.6×10^{13}	1.3×10^{14}	5.4×10^{12}	7.9×10^{13}	8.7×10^{12}	3.4×10^{13}	4.9×10^{14}	1.8×10^{12}
canopy	1.3×10^{9}	6.2×10^{13}	removable	2.5×10^{13}	1.2×10^{14}	5.0×10^{12}	7.4×10^{13}	8.2×10^{12}	1.2×10^{13}	1.8×10^{14}	1.7×10^{12}
			unremovable	3.7×10^{13}	1.8×10^{14}	7.6×10^{12}	1.1×10^{14}	1.2×10^{13}	5.0×10^{13}	7.3×10^{14}	2.5×10^{12}
total canopy	1.7×10^{9}	7.5×10^{13}	removable + defoliation	3.0×10^{13}	1.9×10^{14}	5.5×10^{12}	9.1×10^{13}	1.0×10^{13}	1.6×10^{13}	3.0×10^{14}	1.8×10^{12}
			unremovable	4.4×10^{13}	2.8×10^{14}	8.1×10^{12}	1.3×10^{14}	1.5×10^{13}	5.9×10^{13}	1.1×10^{15}	2.7×10^{12}

[a]PI = prediction interval.

dx.doi.org/10.1021/es401422g | Environ. Sci. Technol. 2013, 47, 9612−9618

defoliated, and 59.3% for evergreen trees. It should be noted that washing by sonication could damage vegetation and the removable fraction could include radionuclides absorbed inside the organ. It should also be noted that there are discrepancies between the washing experiment and real-time situation of washing in the forest canopy. The current washing method has been validated in a previous study,[17] and a previous investigation conducted in the acute phase following Chernobyl reported the removal portion as 25%[18] for evergreen trees, while we found a value of 45%. Taken together, we estimated total uncertainty in the removal portion as 80%; i.e., the uncertainty inherent in our method is a factor of 2. Absorption of radioactivity by trees was qualitatively confirmed by autoradiography (Figure 3). Leaf and needle shapes were clearly observed. In a control measurement using the same species in Kyoto, no radioactive image was observed (data not shown). Therefore, the radioactivity could result from radionuclides emitted from the DNPP. Major emitted radionuclides with short half-lives had disappeared in this study period, and radiocesium was considered a predominant radionuclide. Radioactivity was observed in the leaf blade and veins of a Japanese beech leaf even after washing, suggesting that radioactivity was absorbed by trees. There were many small spots on the needles of Japanese black pine, while the origin remains unclear.

We next estimated the radioactivity trapped by the forest canopy within the 20 km radius. Ambient dose rates were calculated using WRF/CMAQ models, and the trapped amounts were estimated using the relationships between the ambient dose rate and radioactivity in branches or leaves/needles, which were established from observations between radii of 20 and 50 km (panels A and B of Figure 2). The modeled dose rate generally agreed with observed values, as indicated by a correlation coefficient r^2 of 0.78 and an averaged fractional difference f of 0.06 (panels A and B of Figure 4). At 17 of 24 grid points, the air dose rate was reproduced with an error factor less than 2. The error factors at seven other grid points were still less than about 3. The model estimates the fallout on land within the 20 km radius as 10.5×10^{14} Bq, which accounts for 12.2% of the total emissions (8.6×10^{15} Bq)[1] from the crippled plant (see Table S3 of the Supporting Information).

We next estimated the amounts trapped by biomass within the 20 km radius of the Fukushima DNPP. It is estimated that 74.5×10^{12} Bq or 0.86% of the total released has been captured by forest canopy (Table 2). Evergreen trees trapped 62.0×10^{12} Bq of that total. In autumn 2011, 0.7×10^{12} Bq of ^{137}Cs, corresponding to the unremovable portion trapped by leaves of deciduous trees, had fallen onto the forest floor (Table 2). The major portion of the radioactivity, 44.2×10^{12} Bq, is estimated to have already been absorbed by trees and accounts for 0.51% of the total emission (sum of unremovable ^{137}Cs amounts in branchwood of deciduous trees and needles/branchwood of evergreen trees in Table 2).

Because ^{137}Cs has no chemical production or degradation process, except radioactive decay in the atmosphere, the deposition flux calculated by the WRF/CMAQ model is proportional to the emission. The calculated ^{137}Cs amount trapped by biomass is nearly proportional to the air dose rate, which was derived from the modeled accumulated deposition, and consequently, also to the emission. Although the amounts were affected by uncertainty of the emission, the fractional values were not.

There are several sources of uncertainties in this study: (1) uncertainty because of variability of the samples collected in the field survey, (2) model uncertainty, (3) uncertainty in the relationship between the ambient dose rates and the radioactivity of biomass, and (4) uncertainty because of discrepancies between washing experiments and the real-time situation of washing in the forest canopy. We presented uncertainty in the ^{137}Cs amounts because of variability of the samples collected in the field survey and the relationship between ambient dose rates and radioactivities in biomass as a 95% prediction interval (see Figure S2 of the Supporting Information). According to prediction intervals, we incorporated uncertainty in ^{137}Cs radioactivity trapped by canopy in Table 2. We evaluated uncertainty in the modeled dose rates, which was due to uncertainty in the modeled deposition flux, as an error factor less than 3 through comparison to observations (Figure 4B). The fourth uncertainty is estimated to be an error of factor 2, as stated above. To calculate the total uncertainty, the 95% upper and lower predicted intervals for uncertainties 1 and 3 were multiplied by 3 and $^1/_3$ to adjust for uncertainty 2 and obtain upper and lower depositions, 50 or 100% of the removable portion of data obtained in washing experiments was used to calculate uncertainty 4, and the final upper and lower limits were then calculated. The estimates had uncertainties of 3 orders of magnitude.

Our results thus suggest that 0.86% (0.1−16.3%) of all ^{137}Cs released by the Fukushima DNPP has been trapped by biomass. This fraction accounts for 10.7% (1.9−67.2%) of the accumulated amount of ^{137}Cs deposited within the forest in the no-go zone (see Table S3 of the Supporting Information) and is considered to be recycled within the forest in the no-go zone. In the Chernobyl nuclear power plant accident (NPPA), 8.5×10^{16} Bq of ^{137}Cs was estimated to have been released to the environment,[17] which is 9.9 times the amount released from the Fukushima DNPP. Although there is no estimate of the ^{137}Cs fallout on the forest in the Chernobyl NPPA, disappearance rates because of radioactive decay and transport off site for ^{137}Cs in the forest are known to be extremely low and have been estimated to be less than 1% per year.[19] Thus, recycling ^{137}Cs within the forest ecosystem of the no-go zone will occur over the long term in Fukushima, and the zone will be a large ^{137}Cs reservoir. It is difficult to implement effective countermeasures or technology-based decontamination in the forest as in the Chernobyl NPPA. Thus, primitive countermeasures, such as the restriction of activities and the gathering of wild food or firewood, should be implemented for the next 20 years within the no-go zone area in Fukushima.

The current study involves several assumptions and further uncertainties. First, we cannot provide data on the relationships between ambient dose rates and radiation levels in branches or leaves/needles at sites where the air dose rates are greater than 24 μSv/h, which was the maximum value among observed air dose rate levels. Thus, ^{137}Cs trapped by branches and leaves/needles at model grid points within the no-go zone may be underestimated because calculated air dose rates at 2 of the 29 model grid points in this zone were greater than 24 μSv/h. Nevertheless, the unremovable fraction did not increase significantly, only from 0.51 to 0.61%, when the upper limit was not set. Second, ^{137}Cs in forest was assumed to be in an acute phase and not accompanied by recycling in September 2011. These assumptions may again result in the underestimation of ^{137}Cs trapped in biomass.

Human communities in Fukushima are not ecologically separated from the forest, and thus, the fate of ^{137}Cs in the forest will profoundly affect contamination levels in these communities. Long-term monitoring within the forest is needed to elucidate the complex dynamics of radionuclides in biomass, to construct rational decontamination strategies, and to evaluate the effects on human health, agriculture, and the timber industry.

■ ASSOCIATED CONTENT

Supporting Information

Detailed information on calculations, collected samples, the monitoring data set, and additional results. This material is available free of charge via the Internet at http://pubs.acs.org.

■ AUTHOR INFORMATION

Corresponding Author

*Telephone: 81-75-753-4456 (A.K.); 81-774-38-4159 (H.I.). Fax: 81-75-753-4458 (A.K.); 81-774-38-4158 (H.I.). E-mail: koizumi.akio.5v@kyoto-u.ac.jp (A.K.); ishikawa@storm.dpri.kyoto-u.ac.jp (H.I.).

Notes

The authors declare no competing financial interest.

■ ACKNOWLEDGMENTS

This study was supported by an urgent collaborative research grant from the Disaster Prevention Research Institute, Kyoto University (23U-01), the Environment Research and Technology Development Fund of the Ministry of the Environment (ZB-1202), and the Tokyo Kenbikyoin Foundation.

■ REFERENCES

(1) Terada, H.; Katata, G.; Chino, M.; Nagai, H. Atmospheric discharge and dispersion of radionuclides during the Fukushima Dai-ichi Nuclear Power Plant accident. Part II: Verification of the source term and analysis of regional-scale atmospheric dispersion. *J. Environ. Radioact.* **2012**, *112*, 141−154.

(2) Goor, F.; Thiry, Y. Process, dynamics and modelling of radiocaesium cycling in a chronosequence of Chernobyl-contaminated Scots pine (*Pinus sylvestris* L.) plantations. *Sci. Total Environ.* **2004**, *325*, 163−180.

(3) Tobler, L.; Bajo, S.; Wyttenbach, A. Deposition of $^{134,137}Cs$ from Chernobyl fallout on Norway spruce and forest soil and its incorporation in spruce twigs. *J. Environ. Radioact.* **1988**, *6*, 225−245.

(4) Lambert, M. C.; Ung, C. H.; Raulier, F. Canadian national tree aboveground biomass equations. *Can. J. For. Res.* **2005**, *35*, 1996−2018.

(5) *Fukushima Prefecture Forest and Forestry Statistical Yearbook 2010*; Department of Agriculture, Forestry and Fishery, Fukushima Prefecture: Fukushima, Japan, 2011; wwwcms.pref.fukushima.jp/download/1/shinrinkeikaku_toukeisyo22.pdf (in Japanese, accessed June 21, 2012).

(6) Byun, D. W.; Schere, K. L. Review of the governing equations, computational algorithms, and other components of the Models-3 Community Multiscale Air Quality (CMAQ) modeling system. *Appl. Mech. Rev.* **2006**, *59*, 51−77.

(7) Skamarock, W. C.; Klemp, J. B.; Dudhia, J.; Gill, D. O.; Barker, D. M.; Duda, M. G.; Huang, X.-Y.; Wang, W.; Powers, J. G. *A Description of the Advanced Research WRF Version 3*; National Center for Atmospheric Research: Boulder, CO, 2008; NCAR Technical Note NCAR/TN-475+STR, www.mmm.ucar.edu/wrf/users/docs/arw_v3.pdf (accessed June 21, 2012).

(8) *Status of Fukushima Daiichi Nuclear Power Station*; Tokyo Electric Power Company: Tokyo, Japan, 2011; www.tepco.co.jp/en/nu/monitoring/11031501a.pdf (accessed Feb 15, 2013).

(9) *Fukushima Nuclear Accident Analysis Report*; Tokyo Electric Power Company: Tokyo, Japan, 2012; www.tepco.co.jp/en/press/corp-com/release/betu12_e/images/120620e0102.pdf (accessed Feb 15, 2013)

(10) Koizumi, A.; Harada, K. H.; Niisoe, T.; Adachi, A.; Fujii, Y.; Hitomi, T.; Kobayashi, H.; Wada, Y.; Watanabe, T.; Ishikawa, H. Preliminary assessment of ecological exposure of adult residents in Fukushima Prefecture to radioactive cesium through ingestion and inhalation. *Environ. Health Prev. Med.* **2012**, *17*, 292−298.

(11) Slinn, W. G. N.; Hasse, L.; Hicks, B. B.; Hogan, A. W.; Lai, D.; Liss, P. S.; Munnich, K. O.; Sehmel, G. A.; Vittori, O. Some aspects of the transfer of atmospheric trace constituents past the air−sea interface. *Atmos. Environ.* **1978**, *12*, 2055−2087.

(12) Seinfeld, J. H.; Pandis, S. N. *Atmospheric Chemistry and Physics*; John Wiley: Hoboken, NJ, 1998.

(13) Chino, M.; Nakayama, H.; Nagai, H.; Terada, H.; Katata, G.; Yamazawa, H. Preliminary estimation of release amounts of ^{131}I and ^{137}Cs accidentally discharged from the Fukushima Daiichi Nuclear Power Plant into the atmosphere. *J. Nucl. Sci. Technol.* **2011**, *48*, 1129−1134.

(14) *Generic Procedures for Assessment and Response during a Radiological Emergency*; International Atomic Energy Agency (IAEA): Vienna, Austria, 2000; IAEA-TECDOC-1162, www-pub.iaea.org/mtcd/publications/pdf/te_1162_prn.pdf (accessed June 21, 2012).

(15) *Readings of Radioactivity Level Inside of the 20 km Zone of Fukushima Dai-ichi NPP*; Nuclear Regulation Authority: Tokyo, Japan, 2011; http://radioactivity.mext.go.jp/en/list/197/list-1.html (accessed June 21, 2012).

(16) Kasibhatla, P.; Chameides, W. L.; St. John, J. A three-dimensional global model investigation of seasonal variations in the atmospheric burden of anthropogenic sulfate aerosols. *J. Geophys. Res.* **1997**, *102*, 3737−3760.

(17) Wyttenbach, A.; Bajo, S.; Tobler, L. Spruce needles: Standards and real samples. *Fresenius' J. Anal. Chem.* **1993**, *345*, 294−297.

(18) Tobler, L.; Bajo, S.; Wyttenbach, A. Deposition of $^{134,137}Cs$ from Chernobyl fallout on Norway spruce and forest soil and its incorporation into spruce twigs. *J. Environ. Radioact.* **1988**, *6*, 225−245.

(19) United Nations Scientific Committee on the Effects of Atomic Radiation (UNSCEAR). Health effects due to radiation from the Chernobyl accident. In *Sources and Effects of Ionizing Radiation: UNSCEAR 2008 Report to the General Assembly with Scientific Annexes*; United Nations: New York, 2011; Vol. 2, Annex D; www.unscear.org/docs/reports/2008/11-80076_Report_2008_Annex_D.pdf (accessed June 21, 2012).

Chemosphere 93 (2013) 538–544

Contents lists available at ScienceDirect

Chemosphere

journal homepage: www.elsevier.com/locate/chemosphere

Occurrence of perfluorinated carboxylic acids (PFCAs) in personal care products and compounding agents

Yukiko Fujii, Kouji H. Harada, Akio Koizumi *

Department of Health and Environmental Sciences, Kyoto University Graduate School of Medicine, Yoshida, Kyoto 606-8501, Japan

HIGHLIGHTS

- Perfluorinated carboxylic acids (PFCAs) were in personal care products (PCPs).
- The samples list polyfluoroalkyl phosphate esters (PAPs) in their ingredients.
- The concentrations of total PFCAs range from not detected to 19 $\mu g\ g^{-1}$ in PCPs.
- Compounding agents contain high concentrations of PFCAs (35 $\mu g\ g^{-1}$).
- PFCAs are detected in PCPs and compounding agents that use PAPs.

ARTICLE INFO

Article history:
Received 3 December 2012
Received in revised form 6 June 2013
Accepted 16 June 2013
Available online 6 August 2013

Keywords:
Perfluorocarboxylate
Perfluorooctanoic acid
Personal care products
Cosmetics
Polyfluoroalkyl phosphate ester
GC–MS

ABSTRACT

Perfluorinated carboxylic acids (PFCAs), including perfluorooctanoic acid (PFOA), are persistent organic pollutants that pose human health risks. However, sources of contamination and exposure pathways of PFCAs have not been explored. In this study, PFCA concentrations were quantified in personal care products. Among 24 samples that listed fluorinated compounds, such as polyfluoroalkyl phosphate esters (PAPs), in their international nomenclature of cosmetic ingredients (INCI) labels, 21contained PFCAs (13 of 15 cosmetic samples, and 8 of 9 sunscreen samples). The concentrations of total PFCAs ranged from not detected to 5.9 $\mu g\ g^{-1}$ for cosmetics and from not detected to 19 $\mu g\ g^{-1}$ for sunscreens. We also investigated components of PFCAs in cosmetics and sunscreens. Commercially available compounding agents, mica and talc, which were treated with PAPs were analyzed and high concentrations of PFCAs were detected (total PFCAs 2.5 $\mu g\ g^{-1}$ for talc treated with PAPs, 35.0 $\mu g\ g^{-1}$ for mica treated with PAPs). To the best of our knowledge, this is the first report on contamination of end consumer products containing PAPs with high concentrations of PFCAs.

1. Introduction

Perfluorinated compounds are a large group of man-made fluorinated organic chemicals. Perfluorinated alkyl acids such as perfluorooctane sulfonate (PFOS) and perfluorooctanoic acid (PFOA, C8 carbon chain) have been detected in various environmental samples, wildlife, and humans (Houde et al., 2006). In the Stockholm Convention on Persistent Organic Pollutants, PFOS is listed in Annex B (Wang et al., 2009). Fluoropolymer manufacturers have also committed themselves to voluntarily reducing PFOA emissions under a stewardship program of the US Environmental Protection Agency (EPA US, 2006). Temporal trends have revealed decreases in the serum levels of both PFOA and PFOS in the United States, Sweden, Norway, and Japan since 2000 (Olsen et al., 2007; Harada and Koizumi, 2009; Haug et al., 2009; Harada et al., 2010, 2011; Glynn et al., 2012). By contrast, perfluoroalkyl carboxyl acids (PFCAs) with longer carbon chains than PFOA (>C9) have continued to increase in human serum in East Asia and Sweden (Harada et al., 2011; Glynn et al., 2012) and have been detected in human breast milk (Fujii et al., 2012b). Although dietary intakes are generally considered as a major exposure route of long chain PFCAs to humans, the contribution of diet to total human PFCA exposure is still uncertain (D'Hollander et al., 2010; Fujii et al., 2012a). Perfluorinated chemicals have been used in a number of products and significant elevations of serum PFCA levels of those product users were observed in recent studies (Freberg et al., 2010; Nilsson et al., 2010). Several *in vitro* studies have suggested that long chain PFCAs are biologically more toxic than PFOA (Upham et al., 1998; Matsubara et al., 2006; Liao et al., 2009). Therefore, possible exposure routes in humans should be elucidated to establish a rational management policy.

* Corresponding author. Address: Department of Health and Environmental Sciences, Kyoto University Graduate School of Medicine, Yoshida Konoe, Sakyo, Kyoto 606-8501, Japan. Tel.: +81 75 753 4456; fax: +81 75 753 4458.
E-mail address: koizumi.akio.5v@kyoto-u.ac.jp (A. Koizumi).

0045-6535/$ - see front matter © 2013 Elsevier Ltd. All rights reserved.
http://dx.doi.org/10.1016/j.chemosphere.2013.06.049

The direct emissions of long chain PFCAs have been reported for perfluorononanoic acid (PFNA) and perfluoroundecanoic acid (PFUnDA) at 25 t (1 t = 1000 kg) and 7 t, respectively, in 2000 (Prevedouros et al., 2006). In addition, indirect emission of PFCAs could have occurred from precursor compounds, such as fluorotelomer alcohols (FTOHs) and fluoropolymers, for decades (Ellis et al., 2004); (van Zelm et al., 2008). FTOHs are widely produced and used as intermediates for the synthesis of coatings, polymers, and paints (Kissa, 2001). For example, fluorotelomer-based acrylic polymers are used as oil and water repellents. The production of fluorotelomer alcohols was estimated to be approximately 11–14 $\times 10^6$ kg yr^{-1} in 2004 (DuPont Company, 2005).

Recently, polyfluoroalkyl phosphate esters (PAPs), manufactured by a condensation reaction of FTOHs and phosphate, have been widely used in personal care products (PCPs), such as sunscreen and cosmetics for oil and water repellency (Daito Kasei Kogyo., 1993). Biotransformation of PAPs to PFCA has been observed in rats (D'eon and Mabury, 2007) and in a microbial system in wastewater treatment plants (Lee et al., 2010). In addition, technical-grade FTOHs could contain PFCAs as impurities (DuPont Company, 2006). Because of their fate in the ecological system and the manufacturing process, products that use PAPs could contain PFCAs as impurities and/or produce them after degradation. Their application to PCPs could be an exposure source of long chain PFCAs in human serum.

In this study, we investigated the concentrations of PFCAs in PCPs that contained PAPs and some other fluorinated compounds. We also examined commercially available compounding agents of PCPs. The target chemicals included perfluorohexanoic acid (PFHxA), perfluoroheptanoic acid, PFOA, PFNA, perfluorodecanoic acid (PFDA), PFUnDA, perfluorododecanoic acid (PFDoDA), perfluorotridecanoic acid, and perfluorotetradecanoic acid (PFTeDA).

2. Material and methods

2.1. Sample information

We collected PCP samples (sunscreens and cosmetics) that listed PAPs and other fluorinated compounds (e.g. polyfluoroalkyl silylated mica) in their International Nomenclature of Cosmetic Ingredients (INCI) labels. As control samples, a cosmetic (manicure) sample and a sunscreen sample that did not list any fluorinated compounds were collected. A summary of the sample information is provided in Table 1. We obtained 16 commercially available cosmetic samples and 10 sunscreen products distributed by eight different companies. In addition to these end consumer products, we also obtained commercially available compounding agents, including mica and talc, which were treated with PAPs.

2.2. Chemicals

Acetone (LC–MS grade), methanol (LC-MS grade), sodium carbonate (>99.5% pure) and distilled water (LC-MS grade) were obtained from Kanto Chemicals (Tokyo, Japan). Benzyl bromide, tetrabutylammonium hydrogen sulfate, 11H-perfluoroundecanoic acid (11H-PFUnDA) and methyl *tert*-butyl ether (HPLC grade) were purchased from Wako Pure Chemical Industries (Osaka, Japan). A mixture of $^{13}C_2$-labeled PFHxA, $^{13}C_4$-labeled PFOA, $^{13}C_5$-labeled PFNA, $^{13}C_2$-labeled PFDA, $^{13}C_2$-labeled PFUnDA and $^{13}C_2$-labeled PFDoDA were obtained from Wellington Labs (Guelph, Canada). $^{13}C_{12}$- 2,3,3′,5,5′-pentachlorobiphenyl (CB-111) was obtained from Cambridge Isotope Laboratories (Andover, MA).

2.3. Extraction of the PCP samples

Each of the PCPs was subjected to an ion-pair extraction. Approximately 1–200 mg of each PCP, depending on the PFCA concentration, and 500 μL of methanol were placed in a 15 mL polypropylene tube and mixed for 3 h. A recovery surrogate mixture (1 ng each of $^{13}C_2$-labeled PFHxA, $^{13}C_4$-labeled PFOA, $^{13}C_5$-labeled PFNA, $^{13}C_2$-labeled PFDA, $^{13}C_2$-labeled PFUnDA, and $^{13}C_2$-labeled PFDoDA) was added to the tube. Next, 1 mL of 0.5 M tetrabutylammonium/0.25 M sodium carbonate buffer (pH adjusted to 10 using NaOH) and 1 mL of methyl *tert*-butyl ether were added to the samples, and the tubes were vortex mixed for 60 s. The samples were then centrifuged at 9840*g* for 5 min and the organic layer was removed. This step was repeated and the organic layers were combined in a clean glass tube, and then evaporated to dryness under a gentle stream of nitrogen. The residue was redissolved in 100 μL of a 0.1 M benzyl bromide/acetone solution containing 1 ng of 11H-PFUnDA as external calibration standard. The solution was then derivatized at 60 °C for 1 h. No further clean-up was conducted. Derivatized samples were analyzed within 24 h.

2.4. Instrumentation and quantification

Derivatized PFHxA, perfluoroheptanoic acid, PFOA, PFNA, PFDA, PFUnDA, PFDoDA, perfluorotridecanoic acid and PFTeDA were analyzed by gas chromatography-mass spectrometry with electron-capture negative ionization (GC/ECNI/MS) in selected ion monitoring mode (Agilent 6890GC/5973MSD inert, Agilent Technologies Japan, Ltd., Tokyo, Japan). PFCA benzyl esters were separated on a VF-200 ms column (30 m × 0.25 mm i.d., 1 m film thickness; Agilent Technologies Japan, Ltd.) with a helium carrier gas (99.9999% purity; Air Liquide Japan Ltd., Tokyo, Japan). Splitless injections (1 L) were performed with an injector temperature of 220 °C, and the split vent was opened after 1.5 min. The initial oven temperature was 90 °C for 2.25 min, after which it was increased to 135 °C at 1.5 °C min^{-1}, then to 220 °C at 10 °C min^{-1}, and then to 300 °C at 40 °C min^{-1}, and then held at 300 °C for 1 min. Methane (99.9999% purity; Air Liquide Japan Ltd.) was used as the reagent gas (2 mL min^{-1}). The target ions for determination of PFCAs in ECNI are summarized in Table 2.

Standard stock solutions (2 μg mL^{-1}) of native PFCAs (C6 to C14) were diluted to seven working standard solutions (100, 50, 10, 5, 1, 0.5, and 0.1 ng mL^{-1}) using 100 μL of a 0.1 M benzyl bromide/acetone solution with 1 ng of underivatized 11H-PFUnDA and 10 ng of $^{13}C_{12}$-labeled CB111 to monitor the derivatization efficiency. Standard stock solutions (2 μg mL^{-1}) of isotope-labeled PFCAs ($^{13}C_2$-labeled PFHxA, $^{13}C_4$-labeled PFOA, $^{13}C_5$-labeled PFNA, $^{13}C_2$-labeled PFDA, $^{13}C_2$-labeled PFUnDA and $^{13}C_2$-labeled PFDoDA) were also diluted to four working standard solutions (14, 10, 8 and 4 ng mL^{-1}) by 100 μL of a 0.1 M benzyl bromide/acetone solution with 1 ng of underivatized 11H-PFUnDA and 10 ng of $^{13}C_{12}$-labeled CB111. The derivatization efficiency for all PFCA and the 11H-PFUnDA were assumed to be the same. The calibrations were linear and characterized by good correlation coefficients (>0.99). The coefficient of variation of the response ratio (11H-PFUnDA/CB111) was 20% ($N = 10$). The instrumental detection limit was defined as the mass of the analyte producing a peak with a signal-to-noise ratio of three. There is a decrease in detector response of GC–MS measurement depending on chain length of PFCAs. Longer chain PFCAs have smaller detector responses. However, because blank levels were higher for shorter-chain PFCAs than for longer chain PFCAs, the final net instrument detection limits of the shorter and longer chain PFCAs were nearly equivalent (Table 2).